

REPUBLIC OF PERU
REPORT OF GEOLOGICAL SURVEY
THE YAUJA AREA, SOUTHERN PERU

VOL. III
AEROMAGNETIC SURVEY

November 1972

OFFICE OF TECHNICAL COOPERATION AGENCY
MINISTRY OF MINERAL EXPLORATION AGENCY
GOVERNMENT OF JAPAN

REPUBLIC OF PERU
REPORT ON GEOLOGICAL SURVEY
OF
THE YAURI AREA, SOUTHERN PERU

Vol. III

AEROMAGNETIC SURVEY

JICA LIBRARY



1035158[3]

November 1972

OVERSEAS TECHNICAL COOPERATION AGENCY
METALLIC MINERALS EXPLORATION AGENCY
GOVERNMENT OF JAPAN

| | | |
|----------|-----------|------|
| 国際協力事業団 | | |
| 受入 月日 | 84. 3. 19 | 709 |
| 登録No. | 01616 | 66.1 |
| | | KE |

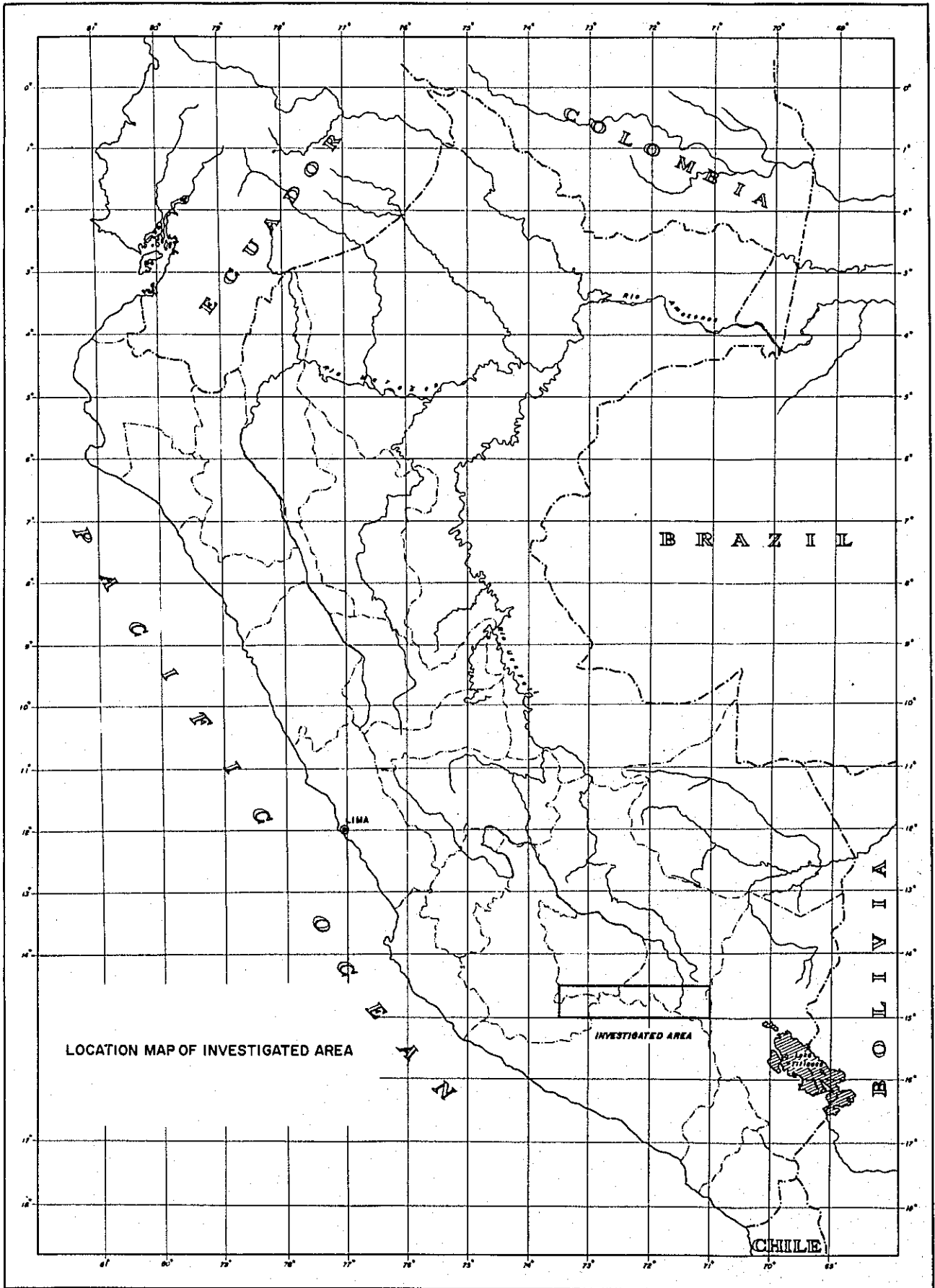
PREFACE

The aeromagnetic survey, forming an integral part of the basic surveys for the development of the natural resources, was conducted in the Yauri area, Southern Peru as a target area of the survey, in 1971 by the Japan's Overseas Technical Cooperation Agency and Metallic Minerals Exploration Agency, based on Japan's cooperation extended to the Republic of Peru for tapping Peruvian natural resources.

The aeromagnetic survey commenced on August 12, 1971, based in Arequipa, Peru, by permission of the Authorities concerned of the Republic of Peru.

The purpose of this survey, combining both photogeological and ground geological surveys, was to clarify the lithology and geological structure of the target area and also to supply the basic informations and data for the development of the mineral resources in Peru.

This report covers from the mentions of, field work of the aeromagnetic survey, data processing, compilation and analytical works, to those of analytical results and geological interpretations. And the report also makes mention of the rock magnetization measurement conducted in connection with the survey.



CONTENTS

PREFACE

| | | |
|-----|--|----|
| 1. | CONCLUSION AND RECOMMENDATION TO THE FURTHER INVESTIGATION | 1 |
| 1-1 | Conclusion | 1 |
| 1-2 | Recommendation to the Further Investigation | 2 |
| 2. | SURVEY DESCRIPTION | 6 |
| 2-1 | Area Description | 6 |
| 2-2 | Survey Programme | 6 |
| 2-3 | Integration of the General Exploration Programme | 6 |
| 3. | SURVEY OPERATIONS | 8 |
| 3-1 | Flight Strips and Base Maps | 8 |
| 3-2 | Flying Operations | 8 |
| 3-3 | Field Crew | 8 |
| 3-4 | Survey Equipment | 8 |
| 3-5 | Field Checking | 9 |
| 4. | ROCK MAGNETIZATION MEASUREMENT | 10 |
| 5. | DATA PROCESSING AND COMPILATION | 12 |
| 5-1 | Path Recovery | 12 |
| 5-2 | Preparation of Magnetic Data | 12 |
| 5-3 | Calcomp Profiles | 12 |
| 5-4 | Control Analysis | 12 |
| 5-5 | Residual Values | 13 |
| 5-6 | Contour Maps | 13 |
| 6. | ANALYSIS ON AEROMAGNETIC MAP | 14 |
| 6-1 | Analysis on Aeromagnetic Map | 14 |
| 6-2 | Digitization of Aeromagnetic Data | 15 |
| 6-3 | Method of Second Vertical Derivatives | 16 |
| 6-4 | Method of Upward Continuation | 18 |
| 6-5 | Analysis on Magnetic Anomaly | 21 |

| | |
|--|----|
| 7. INTERPRETATION | 30 |
| 7-1 General Geology of the Surveyed Area | 30 |
| 7-2 Analysis and Interpretation on Magnetic Data | 33 |
| 7-2-1 Interpretation on the Near-surface Magnetic Component | 34 |
| 7-2-2 Interpretation on the Deep Magnetic Component | 39 |
| REFERENCES | 46 |

ATTACHED MAPS AND FIGURES

| <u>Map No.</u> | <u>Title</u> | <u>Scale</u> |
|-----------------|--|--------------|
| MAP 1-1 & 1-2 | TOTAL MAGNETIC INTENSITY MAP | 1:100,000 |
| MAP 2-1 & 2-2 | TOTAL MAGNETIC INTENSITY MAP | 1:200,000 |
| MAP 3-1 & 3-2 | NEAR-SURFACE MAGNETIC COMPONENT MAP | 1:100,000 |
| MAP 4-1 & 4-2 | NEAR-SURFACE MAGNETIC COMPONENT MAP | 1:200,000 |
| MAP 5-1 & 5-2 | DEEP MAGNETIC COMPONENT MAP | 1:100,000 |
| MAP 6-1 & 6-2 | DEEP MAGNETIC COMPONENT MAP | 1:200,000 |
| MAP 7-1 & 7-2 | INTERPRETATION MAP OF NEAR-SURFACE MAGNETIC COMPONENT | 1:100,000 |
| MAP 8-1 & 8-2 | INTERPRETATION MAP OF NEAR-SURFACE MAGNETIC COMPONENT | 1:200,000 |
| MAP 9-1 & 9-2 | INTERPRETATION MAP OF DEEP MAGNETIC COMPONENT | 1:100,000 |
| MAP 10-1 & 10-2 | INTERPRETATION MAP OF DEEP MAGNETIC COMPONENT | 1:200,000 |
| MAP 11 | AREAS RECOMMENDED TO FURTHER INVESTIGATION | 1:100,000 |

FIGURE 1 - FIGURE 11 : PROFILE A - PROFILE K (1:200,000)

1. CONCLUSION AND RECOMMENDATION TO THE FURTHER INVESTIGATIONS

1-1 Conclusion

- (1) The three-dimensional distribution of magnetic rocks was clarified by this survey and the shallow and deep sub-surface structures were inferred, based on this distribution.
- (2) A great number of magnetic anomalies were observed in the surveyed area, and most of them are thought to be caused by volcanic rocks of the Quaternary period which are distributed on the ground surface or in the near-surface.
- (3) The surveyed area can be tentatively divided into twenty zones, judging from the directions of the axes of the near-surface magnetic bodies as well as the fault lines and magnetic discontinuity lines. In some zones, the magnetic rocks are distributed on the axes of the direction (a) WNW-ESE, and in the other zones, (b) ENE-WSW. And also there are some zones that have no regularity in the direction of their axes. In the western half part of the surveyed area, there are many zones that have such regularity as (a) WNW-ESE, or (b) ENE-WSW.
- (4) It is inferred that there is some relationship between such regularity as mentioned above in (3) and the orogenic movement or the structure, of the Andes, but it is more difficult to infer the relationship between their regularities and the ore deposit, and moreover, it is too difficult to relate the near-surface magnetic rocks distributed on the western half part of the surveyed area (mainly volcanic rocks of the Quaternary period) with the ore deposit.
- (5) In the surveyed area, there also exist many large-scaled magnetic rocks distributed in the deep sub-surface, which cause the anomalies. However, the total number of the rocks is far below that of the near-surface magnetic rocks.
- (6) It is inferred that most of the deep magnetic rocks must be dioritic rocks or granitic diorite, judging from their susceptibility contrast, but there are some regions where they are intruded onto the ground surface or near-surface and cause small-scaled magnetic anomalies.
- (7) In the western two-thirds part of the surveyed area, it is thought that the deep magnetic bodies are arranged in the direction of WNW-ESE and that this arrangement coincides with the structure of the Andes.
- (8) The basin structure as the center of Yauri appears clearly on the aeromagnetic map. As the results of the photogeological analysis, it is found that there are many outcrops of plutonic rocks in this basin and there exist some ore deposits closely related to these plutonics.

- (9) Plutonic rocks which are closely related to the occurrence of ore deposits are distributed much more in the eastern part than the western part of the surveyed area, and it is too difficult to infer the relationship between the plutonic rocks present in the western part and ore deposit, because there are very few exposures of plutonic rocks to the ground surface and the ground surface is almost covered with the Quaternary volcanics.
- (10) The area to be required for the further detailed survey and also the promising area worthwhile the future exploration could be selected, based on the over-all study made on the results of the aeromagnetic and photogeological surveys.

1-2 Recommendation to the Further Investigation

It can be concluded from the interpretations on the results of the aeromagnetic and photogeological surveys that the most potential area where the new ore deposits can be discovered, is Zone II shown in Fig. 1-1 and that there is little possibility of the discovery of new ore deposits in the other zones. And it is possible to limit further the promising areas for the discovery of new ore deposits in Zone II.

It is generally accepted that the existence of acidic or neutral igneous intrusive rocks is needed as the geological environment for the occurrence of these ore deposits, whichever is contact deposit or porphyry copper one.

The magnetic susceptibility of these intrusive rocks is, in general, small, however, the magnetic anomaly is caused by them in case that the sulfide ore deposit is accompanied by magnetite. The special attention should be made to the zone where the magnetic anomaly occur in the marginal part of intrusive rock.

And the presence of limestone is one of the essential prerequisites to the occurrence of contact deposit. From the above viewpoints, the following items should be considered for the selection of the promising area.

- (1) To check the existence of acidic or neutral intrusive rocks.
- (2) Whether the magnetic anomaly is observed above the marginal part of intrusive rock or not.
- (3) Whether there exist the intrusive rocks intruded into limestone or not.
- (4) To choose such zone where the marginal parts extend to the near-surface from the outcrops of intrusive rocks and the magnetic anomalies are observed above the marginal parts.

It is recommendable that, first of all, the detailed ground geological survey should be conducted on the area where the intrusive rocks

are distributed in Zone II of the surveyed area. And furthermore, the promising areas can be delineated, judging from the above-mentioned items (2), (3), and (4), as shown in the MAP 11 "Areas recommended to further investigation".

Especially there exist such big ore deposits as Tintaya and Atalaya in Section 1, and considering the geological environment, Section 1 is the first potential area for the discovery of new ore deposits. The zones marked "Arrow" on the MAP 11 are believed to be such ones where intrusive rock extends to the direction of "Arrow" in the near-surface.

Granitic rock 2-G in Section 2 is supposed to extend further to the west in the near-surface and its marginal part is believed to exist near the "Dotted Line".

In Zone II, it is inferred that the weak or non-magnetic plutonic rocks, which cannot be clarified by the magnetic survey, exist below the ground surface, therefore, the other method of geophysical survey should be used instead of magnetic survey.

In the whole surveyed area excluding Zone II, the magnetic feature in Zone I is similar to that in the basin centering around Yauri, and the distribution of plutonic rock is not found on the surface as a result of the photogeological analysis, however, the existence of the large-scaled plutonic rock is recognized in the deep below the surface as a result of the magnetic survey. This plutonic rock is supposed to extend further to the west outside the surveyed area.

As a result of brief review of the above explanations, the following further surveys are recommended.

- (1) Gravitational survey should be conducted in Zone II, centering around the Yauri Basin, to obtain the informations necessary for the further clarification of the structure of the weak or non-magnetic plutonics or the bed rocks, since this magnetic survey could not satisfied the above clarification.
- (2) Ground geological survey should be made in order to obtain the more detailed informations concerning the geology in Zone II.
- (3) It is interpreted that there is particularly a great possibility of discovering new ore deposit in the delineated sections of 1, 2, 3 and 4 within Zone II. Therefore, it is strongly recommended that the most detailed geological survey should be conducted in these sections.
- (4) The deep electrical survey in Section 1, 2, 3 and 4 is recommended so as to comprehend in detail the three dimensional shape of plutonic rocks distributed on these sections.
- (5) The ground geological survey in Zone I and the aeromagnetic and geological surveys in the uninvestigated area of the west side adjacent to Zone I, would be advisable to be carried out, if the opportunity presents itself.

The above-mentioned Zones and Sections are shown on Fig. 1-1, and Section 1, 2, 3 and 4, are also shown in detail on the MAP 11 "Areas recommended to further investigation" on the scale of 1/100,000.

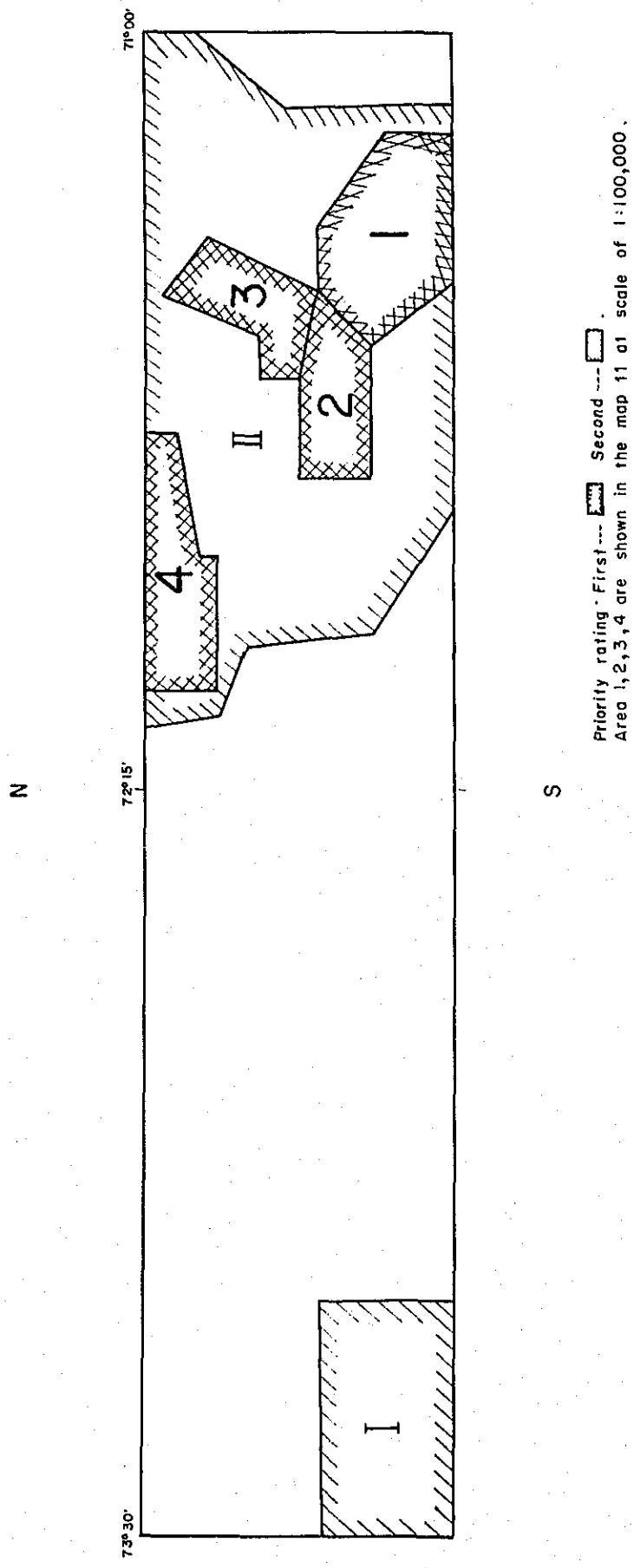


Fig 1-1 AREAS RECOMMENDED TO FURTHER INVESTIGATION

2. SURVEY DESCRIPTION

2-1 Area Description

The survey area, as shown in the Location map, is situated in the southern part of Peru, and forms a rectangular block between latitude 14°30' and 15°00'S, and longitude 71°00' and 73°30'W. The area measures approx. 15,000 square kilometres. The terrain is mountainous. The eastern part is situated in the "alto-plano" region and has an elevation of some 3,900 metres; the western part has mountain peaks up to 5,300 metres high, and is cut by deep gorges and narrow valleys.

2-2 Survey Programme

A survey grid was laid out, with north-south lines 1 km. apart and east-west tie lines 9 kms. apart approximately.

This required 270 lines N-S each 55 kms long: 14,850 line kms
and 7 tie lines E-W each 269 kms long: 1,883 line kms

Total 16,733 line kms

It was decided to fly the whole programme at a constant elevation of 18,500 ft. (5,650 metres approx.) above sea level, so that the data would be continuous over the area, while clearing the peaks safely.

2-3 Integration of the General Exploration Programme

At the planning stage, a phase relations chart was prepared as a reference for the various participants in the aerial and ground work. A generalization of this flow chart, Fig. 2-1, indicates the large degree of inter-dependence of the aerial photographic, photogeological, aeromagnetic and ground geological aspects of the work.

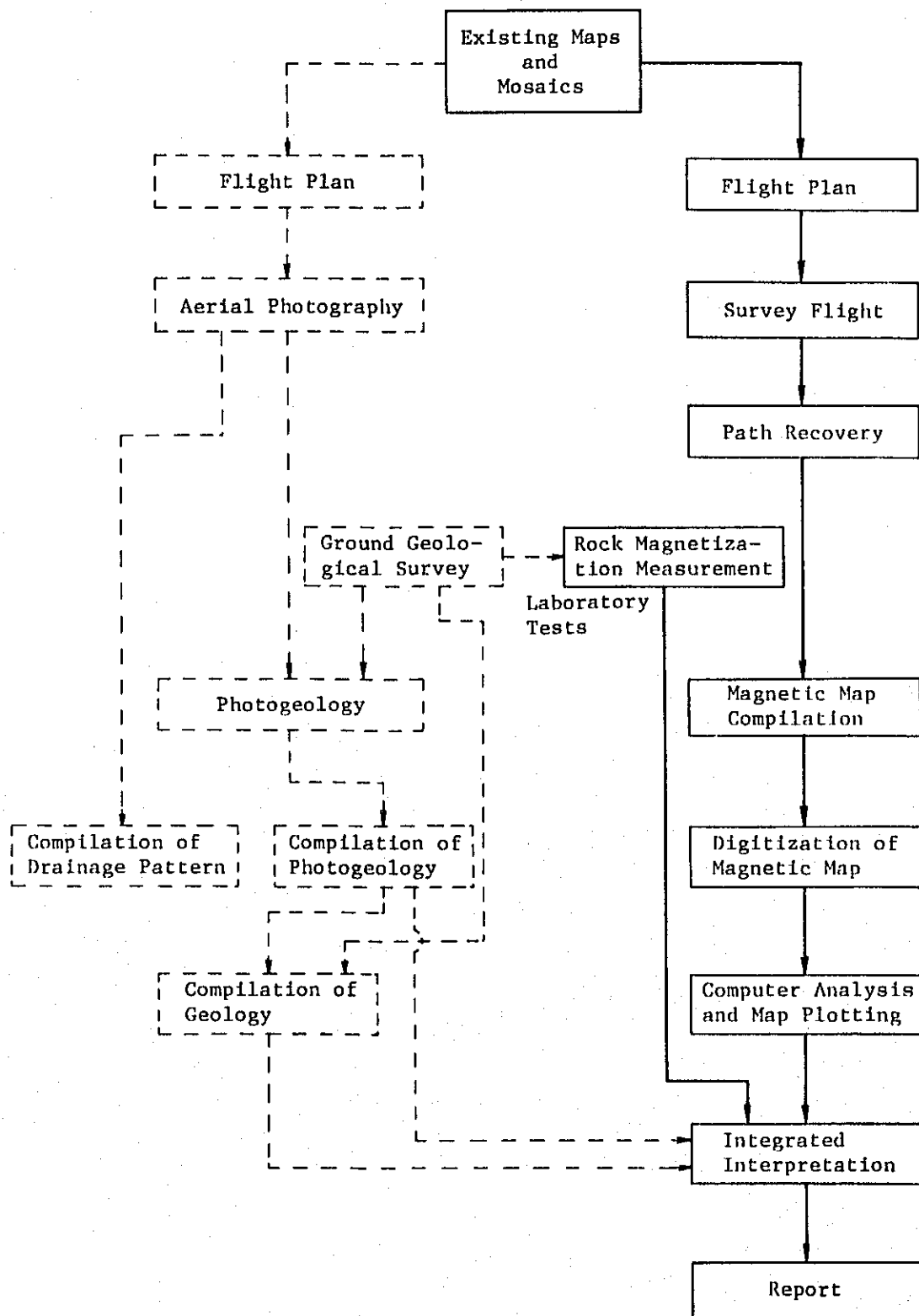


Fig. 2-1 Generalized Flow-Chart

3. SURVEY OPERATIONS

3-1 Flight Strips and Base Maps

It was necessary to use a variety of maps and mosaics or photo indexes obtained from Peruvian government sources for this area. 1/100,000 scale topographic maps were used for all purposes over the area covered between longitude 73°00'W and 73°30'W. The largest scale maps available over the area covered between 72°00'W and 73°00'W were at 1/200,000 and these were used for navigation and, enlarged four times, as base maps for final compilation; uncontrolled photo indexes were used in recovering flight path in this region. Over the area covered between 71°00'W and 72°00'W, photo maps were used for navigation and path recovery, and individual path points were transferred to 1/100,000 topographic maps, which were then used in making the final base maps.

3-2 Flying Operations

When flying started, it was convenient to fly the tie lines from Juliaca east of the survey area, and these were completed in two flights on August 19 and 20, 1971. For the rest of the work, Arequipa, which lies south of the survey area, was a more convenient base since it is at a much lower elevation and less affected by clouds. The crew moved on Aug. 21-22 and recommenced flying on Aug. 24. Production was held up principally by clouds and severe turbulence, which forced premature ending of a number of flights. The flying was completed on Sept. 20. Diurnal magnetic variations did not delay the survey.

3-3 Field Crew

The survey was carried out by the following men:

| | |
|-----------------------|--------------|
| Party Chief | I. Gaüzere |
| Assistant Party Chief | A. Cassin |
| Data Man | N. Krumm |
| Pilot | W. Beaumont |
| Co-Pilot | N. Spraggs |
| Electronics Operator | J.C. Poirier |
| Engineer | K. Proctor |

3-4 Survey Equipment

The survey aircraft was a Douglas DC-3, registration N 151 D. It carried a caesium-vapour magnetometer in a bird, suspended by cable below the aircraft to remove it from extraneous magnetic fields. This instrument measures the total intensity of the earth's magnetic field in units of 0.01 gammas at one second intervals, controlled by a crystal clock. This clock controlled fiducial marks, added simultaneously to all records. The measurements were recorded digitally on magnetic tape, and also in

analog form for monitoring purposes. The analog record was made on chart paper, ten inches wide, with steps automatically made at integral 100 gamma readings. A second channel on the analog record showed altitude changes, measured by a Rosemount barometric altimeter. The aircraft also carried a Bendix Doppler system used to assist navigation. The digital magnetic tapes recorded time and magnetometer measurements, together with altimeter and Doppler along and off-track values. Exact flight path was recorded on 35 mm. film by two tracking cameras, continuous strip and single-frame.

A similar magnetometer was operated at the flying base to record time-variations of the magnetic field in analog and digital form. Airborne and ground magnetometer measurements were synchronised by the crystal clocks, checked together before each flight.

3-5 Field Checking

After each survey flight, the analog records were checked for data quality and edited. Tracking film was developed and flight path located on the maps or mosaics and checked.

4. ROCK MAGNETIZATION MEASUREMENT

Some rock samples were taken from the surveyed area by the ground geological survey team for the reference of analysis on the aeromagnetic data. The locations where the samples were taken are shown on the MAP 7-1 and 7-2 "Near-surface magnetic component map".

The lithology and magnetic susceptibility of the rock samples are shown on Table 4-1. The susceptibility measurements were made, using a magnetic susceptibility meter, Bison Instruments Model 3101 owned by Sumiko Consultants Co., Ltd.

The rock samples can be tentatively classified as andesitic rocks, granitic rocks, tuffs, and marine sedimentary rocks. Their number and the average values of their susceptibilities are shown as follows.

| | | | |
|--------------------------|---------|-----------------------|----------------|
| Andesitic rocks | 17 pcs. | 0.88×10^{-3} | c.g.s.e.m.u/cc |
| Granitic rocks | 11 pcs. | 1.22×10^{-3} | " |
| Tuffs | 7 pcs. | 0.13×10^{-3} | " |
| Marine sedimentary rocks | 7 pcs. | 0.07×10^{-3} | " |

It is clear that the magnetism of andesitic rocks and granitic rocks is stronger than that of the other two types of rock. The magnetism of granitic rocks measured at this time is supposed to be a little stronger than that of an ordinary type of these rocks, but it is inferred that granitic rocks include dioritic rocks.

It is supposed that it is difficult to interpret the magnetism of rocks distributed on the whole area, because three quarters of rock samples were taken in the eastern part of the surveyed area. However, it is possible to estimate roughly the magnetism of the rocks in the area, based on the average values as mentioned above.

Table 4-1 Susceptibilities of the Rocks Sampled in the Survey Area

| Sample No. | Susceptibility ($\times 10^{-3}$ c.g.s.e.m.u/cc) | Lithology | Layer |
|------------|--|----------------------------|-------|
| * A-1 | 2.18 | Granite | 3 |
| -2 | 0.02 | Tuffaceous dacite | 2 |
| -3 | 0.23 | Andesite flow | 2 |
| -4 | 0.53 | Andesite | 2 |
| -6 | 0.84 | Andesitic volcanic breccia | 2 |
| -7 | 0.05 | Tuff breccia | 2 |
| -8 | 2.26 | Basalt flow | 1 |
| -9 | 1.13 | Basalt lava | 1 |

| Sample No. | Susceptibility (x 10 ⁻³ c.g.s.e.m.u/cc) | Lithology | Layer |
|------------|---|-------------------------|--------|
| A-10 | 0.28 | Andesitic volcanic flow | 2 |
| -11 | 0.30 | Tuff | 1 |
| -15 | 0.87 | Andesite | 2 |
| K- 2 | 0.03 | Limestone | 4 |
| - 6 | 0.09 | Granite | 3 |
| - 8 | 0.24 | Andesite agglomerate | 2 |
| -15 | 0.27 | Dacitic tuff | 2 |
| -15' | 1.13 | Andesite | 2 |
| -19 | 2.74 | Andesite | 2 |
| -29 | 0.05 | Tuff | 1 |
| -30 | 0.12 | Caleareous tuff | 4 |
| -31 | 1.76 | Granite | 3 |
| -34 | 0.05 | Andesite | 2 |
| T- 1 | 0.13 | Red tuff | 1 |
| - 2 | 0.03 | Quartzite | 4 |
| - 3 | 0.01 | Limestone | 4 |
| - 4 | 0.03 | Diorite | 3 |
| - 5 | 0.02 | Sandy tuff | 1 |
| - 6 | 2.22 | Sandstone | 5 |
| - 7 | 0.02 | Tuffaceous shale | 1 |
| - 8 | 0.98 | Sandstone conglomerate | 2 |
| - 9 | 0.36 | Sandstone | 2 |
| -10 | 0.03 | Siltstone | 1 |
| -11 | 0.07 | Granitic rock | 3 |
| S- 1 | 0.36 | Granitic rock | 3 |
| - 2 | 0.03 | Andesite | 2 |
| - 3 | 1.55 | Quartz porphyry | 1 |
| - 4 | 0.11 | Andesite | 2 |
| - 5 | 1.29 | Andesite | 2 |
| - 6 | 0.69 | Granitic rock | 4 or 3 |
| * - 7 | 1.94 | Granitic rock | 3 |
| - 8 | 0.03 | Granitic rock | 3 |
| - 9 | 0.03 | Sandstone | 4 |
| -10 | 4.73 | Dioritic porphyry | 3 |

Note: Layer 1. Quaternary 4. Lower Mesozoic
2. Tertiary 5. Paleozoic
3. Upper Mesozoic

Rocks indicated by the symbol (*) are not shown in Maps because they were sampled outside the surveyed area.

5. DATA PROCESSING AND COMPILATION

When the data had been received in Ottawa, it was compiled to create two final products: total magnetic intensity contour maps, and Calcomp profile plots. The processing followed routines described.

5-1 Path Recovery

The exact points of intersection of each line and tie line were identified by crossing pairs of 35 mm. tracking film. In addition, points were identified from the tracking film onto the base maps. All locations were then digitized, according to a standard UTM (Universal Transverse Mercator) grid. The digitized flight path was then checked by calculating the aircraft ground speed between intersections and other key points. Erratic speeds were checked, and the sources of error identified and eliminated.

5-2 Preparation of Magnetic Data

The magnetometer measurements, both airborne and ground were checked and edited to ensure accuracy and completeness. The ground values were subtracted from air values to eliminate time variations of the field as much as possible. Since the resultant differences were close to zero, an arbitrary constant of 26,000 gammas was added to restore them to figures approaching the original measurements. At this stage, the data were treated with a non-linear filtering operator to remove any noise spikes.

5-3 Calcomp Profiles

Profiles of the "air minus ground" values of each line were made by a 30 inch Calcomp plotter showing two traces of total magnetic intensity and one of vertical gradient. To eliminate regional effects an end-to-end linear regional was applied to the total intensity values setting the start and end values of each line at the same level. The two traces are different in vertical scale only, using 20 gammas per inch as a fine scale and 50 gammas per inch as a coarse scale. Because of strong anomalies on the tie lines and on lines 83-143, the coarse scale was set at 100 gammas per inch. Vertical gradients were calculated using the operators developed by H. Naudy of CGG (Compagnie Générale de Géophysique), using a differencing interval of 3 seconds and plotting at a scale of 0.0952 gammas per foot per inch.

5-4 Control Analysis

In order to level the data together, the "air minus ground" values at each intersection were located on both lines and tie lines. The line minus tie line (L-T) differences were analysed graphically to arrive at a smooth pattern of adjustments. Erratic differences were checked and corrected.

5-5 Residual Values

The air minus ground magnetic values on each line and tie line were then ready for final assembly and adjustment as residual values. Adjustments were applied for -

- a) control analysis as described above
- b) regional correction calculated from the IGRF (International Geomagnetic Reference Field) by linear interpolation in two directions from the following IGRF values:

| | | |
|-------|-------|--------------|
| 14° S | 74° W | 27130 gammas |
| 14° S | 72° W | 26895 " |
| 16° S | 72° W | 26490 " |
| 16° S | 74° W | 26750 " |

- c) since subtraction of the IGRF again brought the magnetic values close to zero, an arbitrary constant of 10,000 gammas was added to keep all final residual values positive.

With these adjustments final residual values were calculated throughout the survey at 2.5 second intervals along the lines flown, together with geographic VTM co-ordinates. They were then transcribed onto a set of 1/50,000 scale maps.

5-6 Contour Maps

The transcribed residual values were contoured, using an interval of 0.5 gammas wherever feasible, and drafted to make the ten final magnetic contour maps. The final sheets were photographically reduced and composited to scales of 1/100,000 and 1/200,000.

6. ANALYSIS ON AEROMAGNETIC MAP

6-1 Analysis on Aeromagnetic Map

Magnetic anomalies shown on an "aeromagnetic map" are caused by the induced magnetic field which is attributed to the rocks present above and below the ground surface, their rocks being magnetized by the earth's magnetic field, and caused by remanent magnetization of the rocks. The strength of the induced magnetic field is in proportion to the magnitude of the rock's susceptibility. For this purpose, the magnetic anomalies were analyzed, assuming that the remanent magnetization was negligibly small and they were caused by the induced magnetic field only.

The surveyed area has approx. minus 4° of magnetic inclination, therefore the negative magnetic anomaly appears almost right above the magnetic body due to the induced magnetization.

At a glance over the aeromagnetic map, it is easily understood that there are differences in the degree of the crowd of the magnetic anomaly, its shape, its size of scale and so on, which reflect the differences of the geological conditions.

Practically speaking, a model's curve suitable to the individual anomaly is selected and then the depth, shape, size and susceptibility contrast, of the magnetic body causing its anomaly, are quantitatively calculated.

To make further detailed analysis, the calculations are made through various mathematical filters. However, for this analysis, the calculations were made through two types of mathematical filter of the "second vertical derivative method" and the "upward continuation's method" in order to separate the "near-surface magnetic component" from the "deep magnetic component".

By the "second vertical derivative map", a small anomaly concealed behind the anomaly of long wave-length and of big amplitude, can be detected, and the boundary of a small-scaled magnetic body can also be detected.

And by the "upward continuation", the amplitude of an anomaly having short wave-length is attenuated and the anomaly caused by a large-scaled magnetic body can be detected. Upward map is also quantitatively analysed.

Such qualitative and quantitative analytical results are studied in combination with geological informations and other data available for this purpose, and then the sub-surface structural maps are drawn.

The process of such analytical works is shown on Fig. 6-1 as a flow chart.

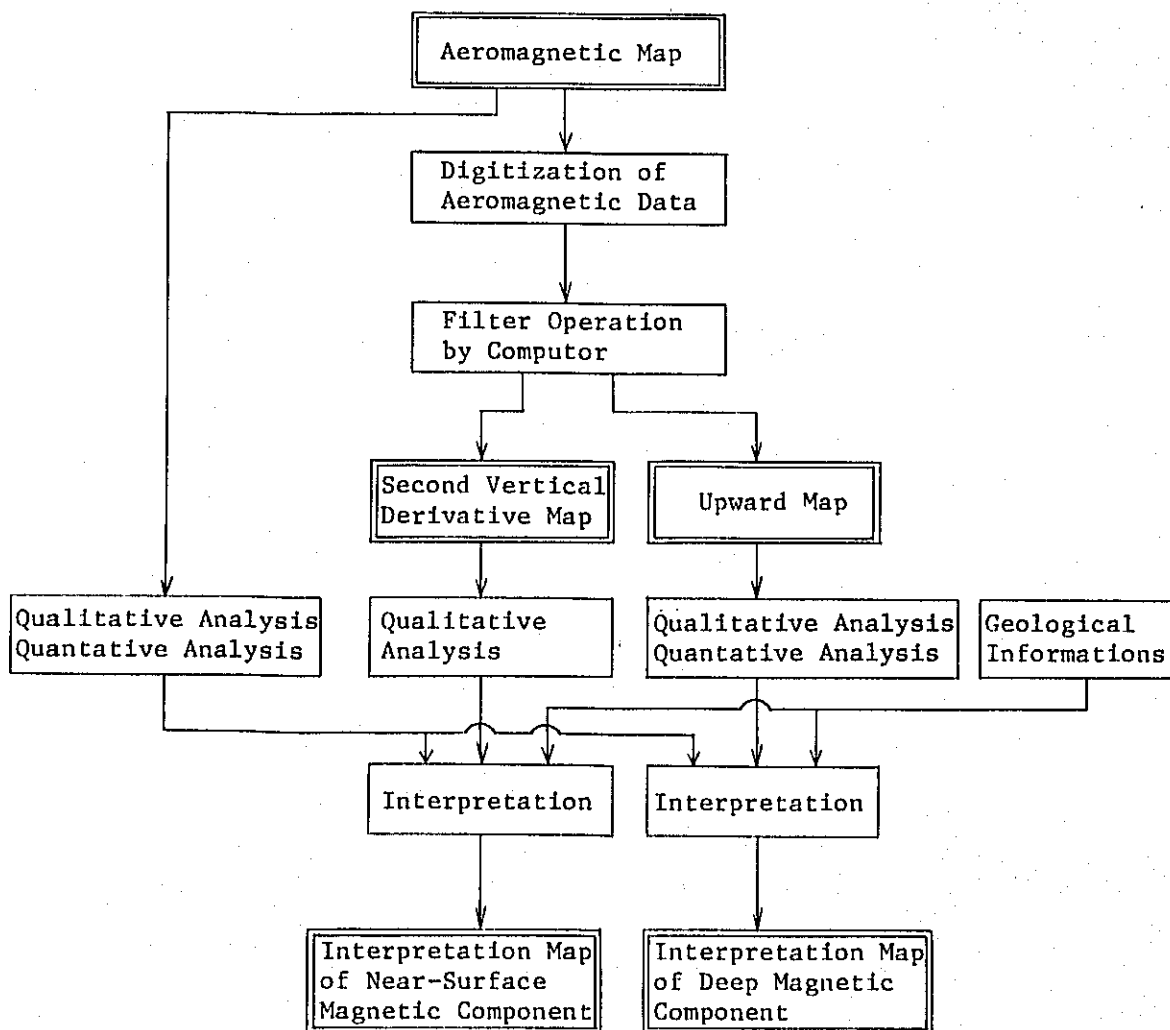


Fig. 6-1 Flow-Chart of Analytical Works on Aeromagnetic Map

6-2 Digitization of Aeromagnetic Data

Aeromagnetic data are digitized on a square grid to pass these data through mathematical filters of the second vertical derivative method and the upward continuation.

The 1/50,000 scale aeromagnetic maps were digitized on a square grid at an interval of 1 kilometer (2 cm. grid on map). The digitization was made to the unit of 0.1 gamma, on the grid points of 56 by 272, i.e. totaling 15,232. Grid point (1,1) was taken as the origin at latitude 14°30'07"S and longitude 73°29'58"W.

6-3 Method of Second Vertical Derivatives

The method of second vertical derivatives is characterized as high pass filter which amplifies the short period component and attenuates the long period component, of magnetic anomaly.

Therefore, to extract the near-surface magnetic component, the method of second vertical derivatives was applied to the aeromagnetic map.

Second vertical derivative map was prepared, using mainly Rosenbach's formula (1) as shown below and also Henderson & Zietz's formula (2) being applied to the circumference as shown below.

$$\frac{\partial^2 \Delta T}{\partial Z^2} = \frac{1}{S^2} \cdot \frac{1}{24} (96\Delta T_0 - 72\Delta T_1 - 32\Delta T_2 + 8\Delta T_4) \dots\dots\dots (1)$$

$$\frac{\partial^2 \Delta T}{\partial Z^2} = \frac{2}{S^2} (3\Delta T_0 - 4\Delta T_1 + \Delta T_2) \dots\dots\dots (2)$$

where

$$\Delta T_1 = \frac{\Delta T_{11} + \Delta T_{12} + \Delta T_{13} + \Delta T_{14}}{4}$$

$$\Delta T_2 = \frac{\Delta T_{21} + \Delta T_{22} + \Delta T_{24}}{4}$$

$$\Delta T_4 = \frac{\Delta T_{41} + \Delta T_{42} + \Delta T_{43} + \Delta T_{44} + \Delta T_{45} + \Delta T_{46} + \Delta T_{47} + \Delta T_{48}}{8}$$

and each location of ΔT_{11} , ΔT_{12} , ΔT_{48} is shown on Fig. 6-2.

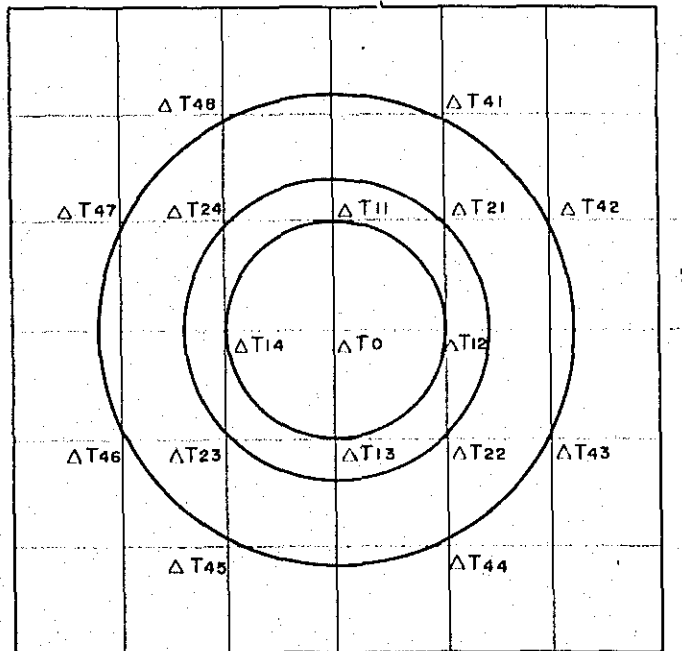


Fig. 6-2 Location of Points on the Grid for the Computation of Second Vertical Derivatives

The calculation was made with regard to each point at such 1 km interval on the grid as digitized in 6-2 above, based on $S = 1$ km and using the formula (1) and (2).

The frequency response of the method of second vertical derivatives is shown on Fig. 6-3.

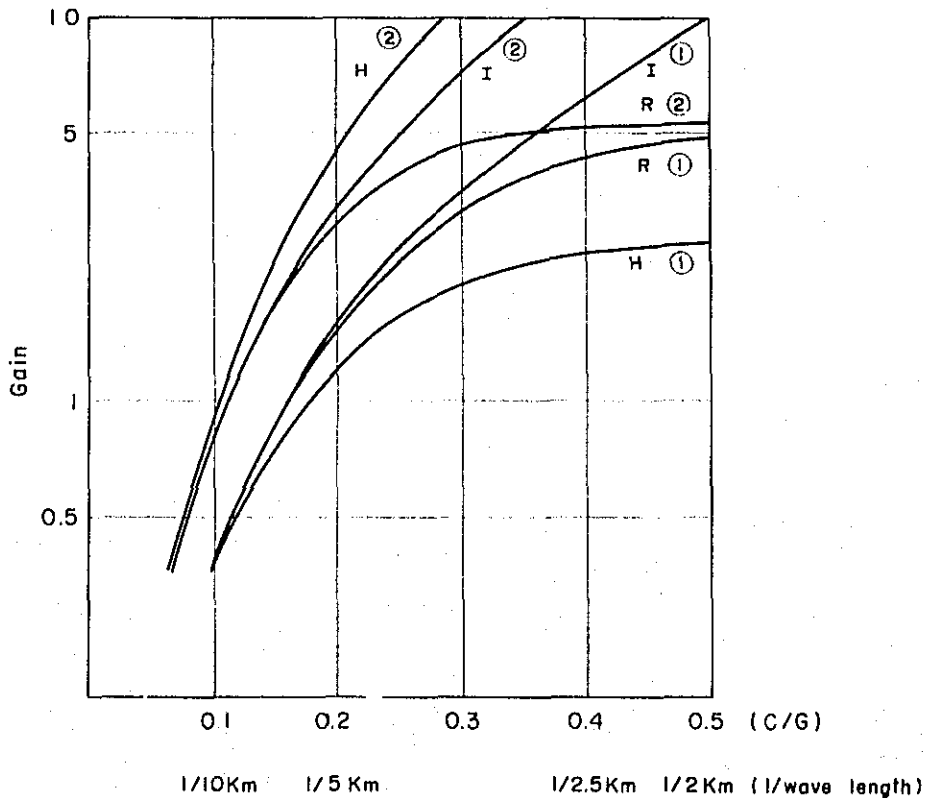


Fig. 6-3 Frequency Response of Second Vertical Derivative Method

"I" indicates the curve by "theoretical second vertical derivatives".

"R" indicates the curve by "Rosenbach's formula".

"H" indicates the curve by "Henderson & Zietz's formula".

① indicates the degree of attenuation dependent on C/G of south-north direction (or east-west direction) in the case of C/G of the east-west direction (or south-north direction) of magnetic anomaly, being equal to zero.

② indicates the degree of attenuation dependent on C/G in the case of C/G of east-west direction of magnetic anomaly being the same as that of south-north direction (magnetic anomaly shaping a complete circle).

In this operation, the degree of attenuation of magnetic anomaly depends on the component following the grid direction (the components of south-north direction and east-west direction) of anomaly's "cycles/grid interval" (hereinafter called "C/G"), namely, it can be said that it depends on the size and shape of anomaly.

From Fig. 6-3, it is understood that, by the calculations made according to Rosenbach's formula used for this analysis, the short period anomaly of C/G exceeding approx. 0.4, namely, less than approx. 2.5 km of wave length, is amplified approx. fivefold and that anomaly of C/G equal to 0.1, namely, approx. 10 km of wave-length, is attenuated to about half.

The following second vertical derivative maps are attached hereto.

MAP 3-1, 3-2 (1/100,000 scale)

MAP 4-1, 4-2 (1/200,000 scale)

From these second vertical derivative maps, it is understood that short period magnetic anomaly, which is thought to be caused by a small-scaled near-surface magnetic rock body, has been amplified and appeared as an independent anomaly and that long period magnetic anomaly, which is thought to be caused by a large-scaled deep magnetic rock body, has attenuated. And these maps served as an effective analysis on "near-surface magnetic component" with the use of original aeromagnetic map.

6-4 Method of Upward Continuation

The method of upward continuation is used to easily obtain a big contour pattern in magnetic map, through the attenuation of the short period magnetic anomaly which is thought to be caused by a small-scaled near-surface magnetic rock body, and through the amplification of the long period magnetic anomaly. Therefore, it was used for the extraction of anomaly caused by deep magnetic component.

From the aeromagnetic map (the height of horizontal flight: 5,650 m above sea level), the aeromagnetic map at the level of 6,650 m above sea was made by the method of upward continuation.

The method of $(\sin X)/X \cdot (\sin Y)/Y$ expanded into the third dimension by Tsuboi and Tomoda was applied to the upward continuation.

As a matter of practice, the calculation was made by the method of convolution, namely, the values of (9 x 9) grid points digitized at 1 km interval, as in 6-2 above, are multiplied by Mufti's coefficients of upward continuation given by (9 x 9) grid matrix, as shown on Fig. 6-4, and then added together. The total sum figured out after adding up as above amounts to the magnetic values of 6,650 m above sea level, calculated on the basis of the values of 5,650 m above sea level, by the method of upward continuation. The coefficients of $d = 1.0S$ ($S = 1$ km) are used herein. The difference of elevation between the original map (5,650 m) and upward map (6,650 m) amounts to 1 kilometer, the same figure of the grid interval.

| | | | | | |
|-----|----------|----------|----------|----------|----------|
| (4) | 0.002067 | 0.002266 | 0.001943 | 0.001402 | 0.000987 |
| (3) | 0.006922 | 0.005412 | 0.003552 | 0.002263 | 0.001402 |
| (2) | 0.014563 | 0.012146 | 0.006917 | 0.003552 | 0.001943 |
| (1) | 0.069934 | 0.038218 | 0.012146 | 0.005112 | 0.002266 |
| (0) | 0.160836 | 0.069934 | 0.014563 | 0.006922 | 0.002067 |
| | (0) | (1) | (2) | (3) | (4) |

Fig. 6-4 Coefficients of Upward Continuation

The frequency response of the upward continuation is shown on Fig. 6-5. The degree of attenuation of magnetic anomaly depends on the components of south-north direction and east-west direction, of C/G, as is the same case with the second vertical derivatives.

From this figure, it is understood that, calculated on the basis of Mufti's coefficients, the anomaly having long wave-length, namely, a small value of C/G, is not attenuated, but, on the contrary, even the anomaly having a large value of C/G is attenuated only approximately half. Therefore, the anomaly having a bigger amplitude among short period anomalies remains on the "upward continuation map". The anomaly which attenuates most, is the one in the case of C/G being equal to approx. 0.2, namely, wave-length being equal to approx. 5 km.

The following upward maps thus made are attached hereto.

MAP 5-1, 5-2 (1/100,000 scale)
 MAP 6-1, 6-2 (1/200,000 scale)

From these upward maps, it is understood that the anomalies, which are thought to be caused by small-scaled near-surface magnetic rock bodies, have attenuated, provided, however, that, as stated above, the short period anomalies have attenuated, but larger ones in amplitude have still remained, and that the long period anomalies, which are thought to be caused by a large-scaled deep magnetic rock bodies, have remained. Therefore, these upward maps were useful to infer the deep sub-surface structure.

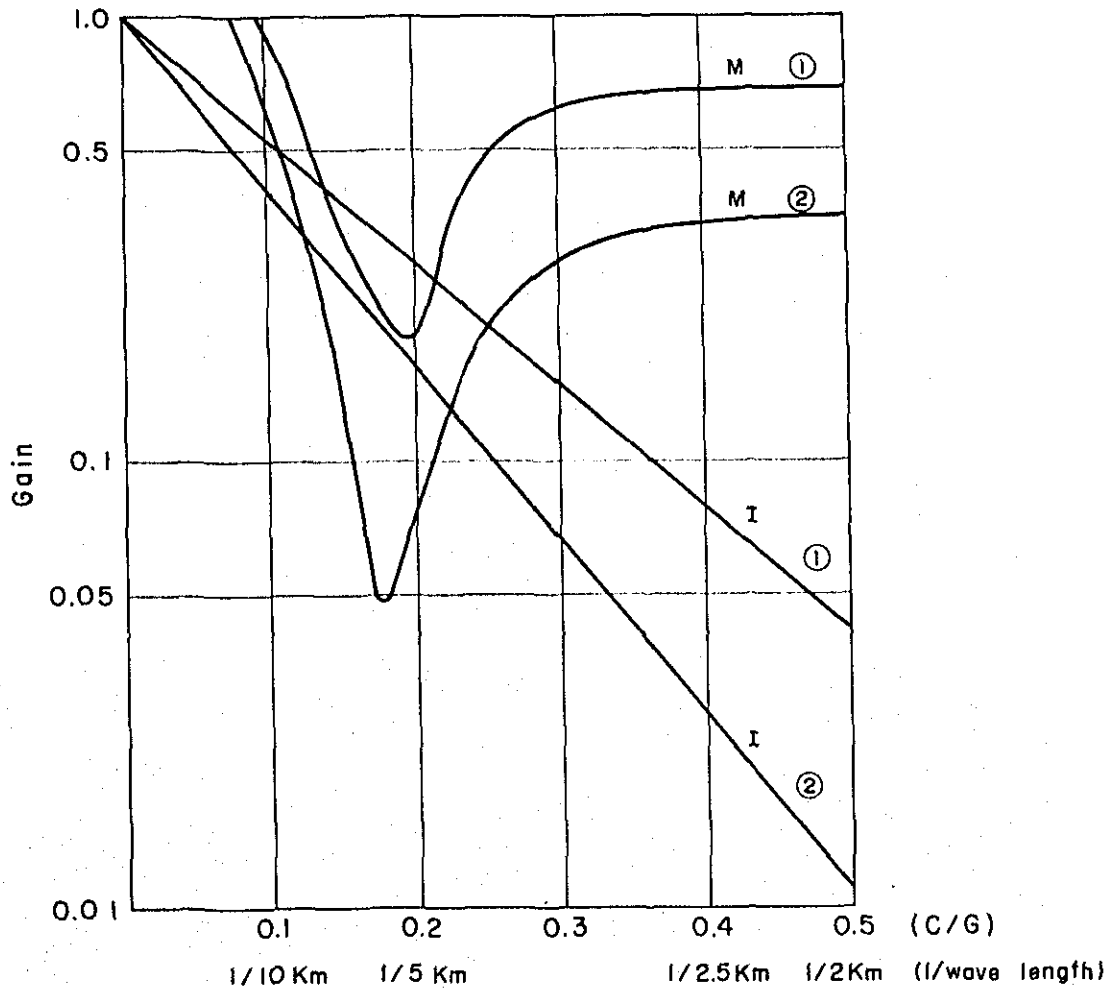


Fig. 6-5 Frequency Response of Upward Continuation

"I" indicates the curve by "theoretical upward continuation".

"M" indicates the curve by "Mufti's formula".

① indicates the degree of attenuation depending on C/G of south-north direction (or east-west direction) in the case of C/G of east-west direction (or south-north direction) of the anomaly, being equal to 0.05.

② indicates the degree of attenuation depending on C/G in the case of C/G of east-west direction and south-north direction of the magnetic anomaly being the same (the magnetic anomaly shaping a complete circle).

6-5 Analysis on Magnetic Anomaly

From the analysis on individual magnetic anomaly, the shape, size, depth below the surface, and susceptibility contrast, of the magnetic rock body causing such magnetic anomaly, can be detected.

The method of "curve matching" was mainly used for the analysis on magnetic anomaly and the use of "specific point method" was combined as the case might be. The method of curve matching is to determine the above-mentioned various elements of a magnetic rock body by means of collating the observed curve with anomaly curves — so-called standard curves — calculated on the various models, and then selecting the most suitable model.

The calculations on the models were made as magnetic inclination of minus 5°. The patterns of magnetic anomalies and their profiles calculated on several prism models are shown on Fig. 6-6 to Fig. 6-10. And the profile of magnetic anomaly caused by dyke-shaped structure, that by step-shaped structure, and that by sheet-shaped structure, are shown on Fig. 6-11, 6-12 and 6-13, respectively.

For this analysis, the standard curves calculated on the prism models, within which magnetization is uniform, were mainly used, and those calculated on the dyke models or step models etc. were applied if necessary.

From this curve matching method, the shape, size, depth, and susceptibility contrast of the magnetic body causing the individual magnetic anomaly appeared on the aeromagnetic map and upward map, were obtained. And moreover, susceptibility contrast, " ΔK ", was obtained from the following formula.

$$\Delta K = \frac{1}{T_0} \cdot \frac{\Delta T_0}{\Delta T_m} \quad \text{c.g.s.e.m.u./cc}$$

where $T_0 = 27,000^{\gamma}$ (The average value of total magnetic intensity covering the surveyed whole area.)

ΔT_0 indicates the magnetic amplitude of anomaly observed

ΔT_m indicates the magnetic amplitude of anomaly by the model collated. (In this case, the calculation was made by the total magnetic intensity value of 1^{γ})

The interpretation on the sub-surface structure made by collating the individual anomaly with geological informations is written in Chapter 7.

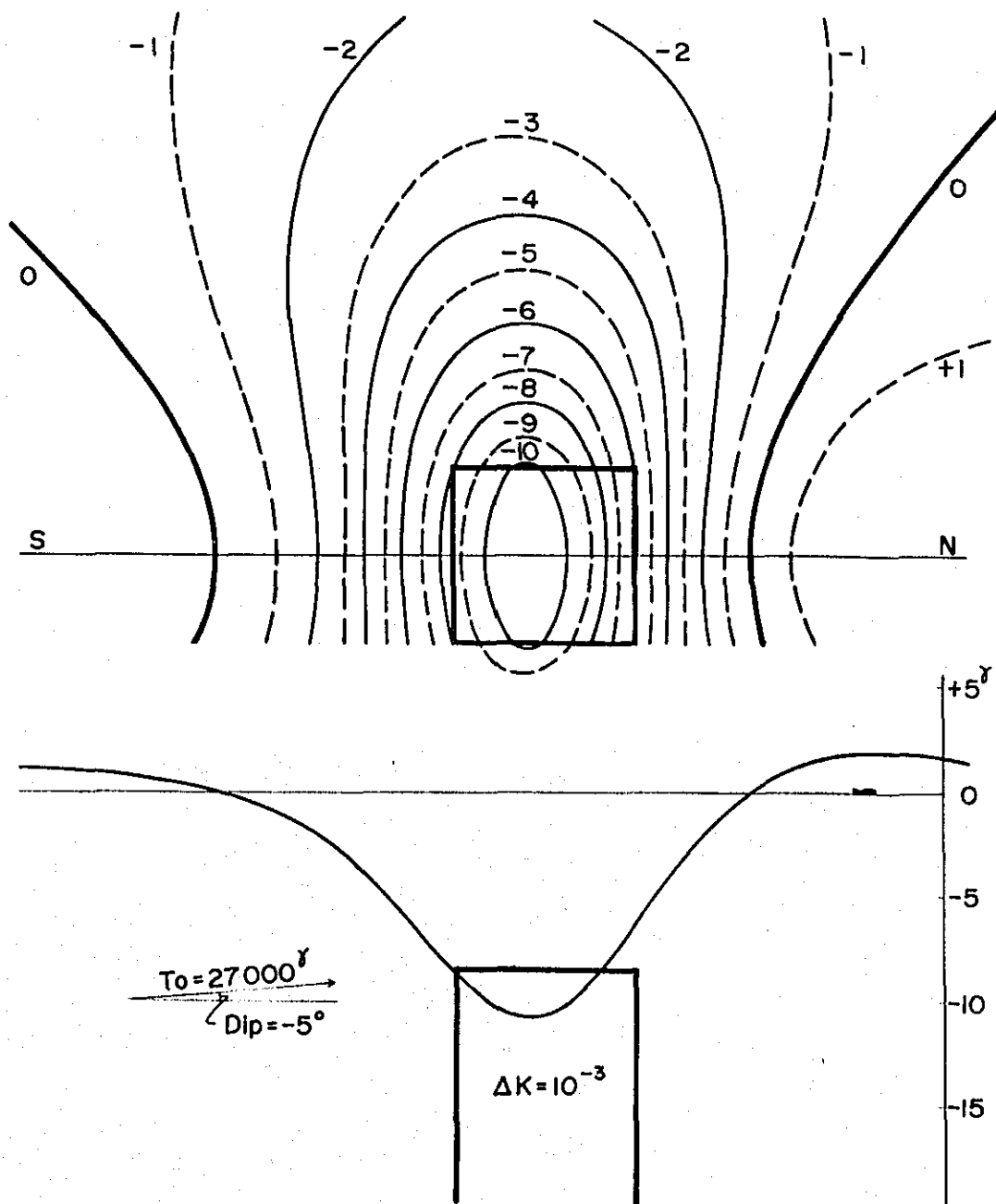


Fig. 6-6 Total magnetic anomaly by a prism model

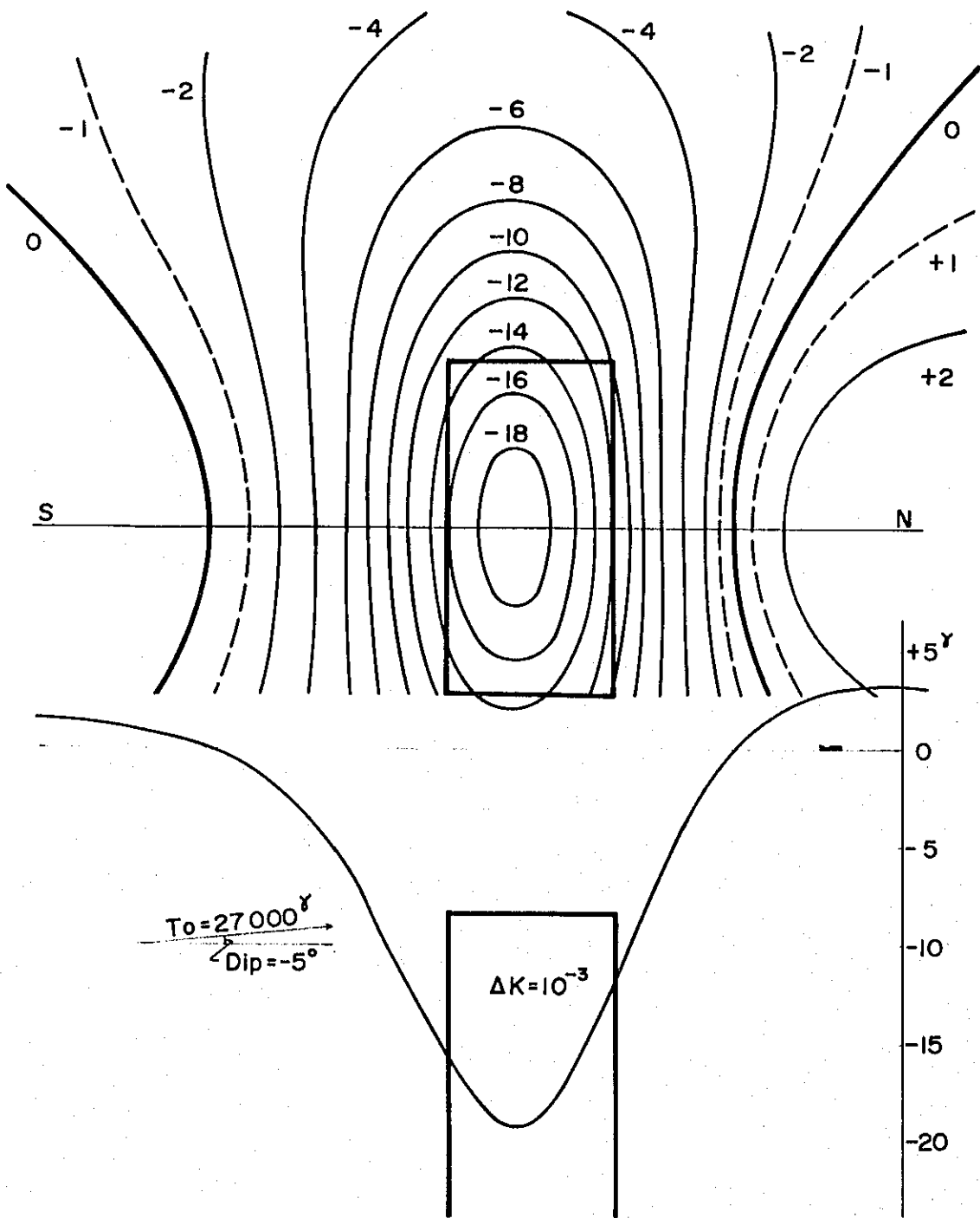


Fig. 6-7 Total magnetic anomaly by a prism model

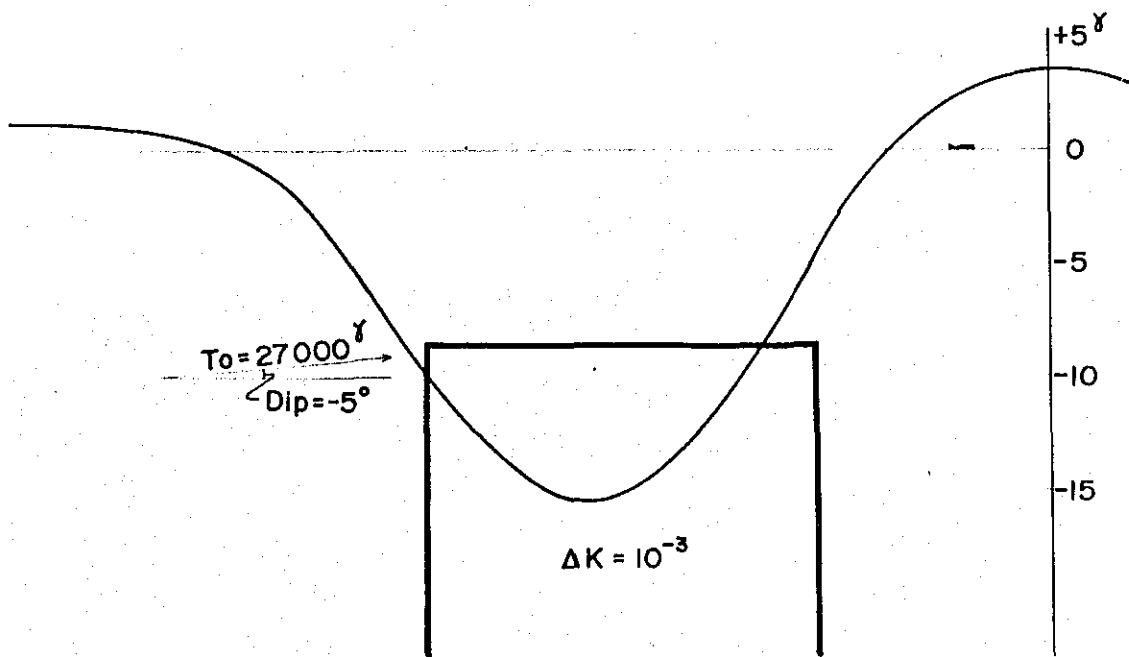
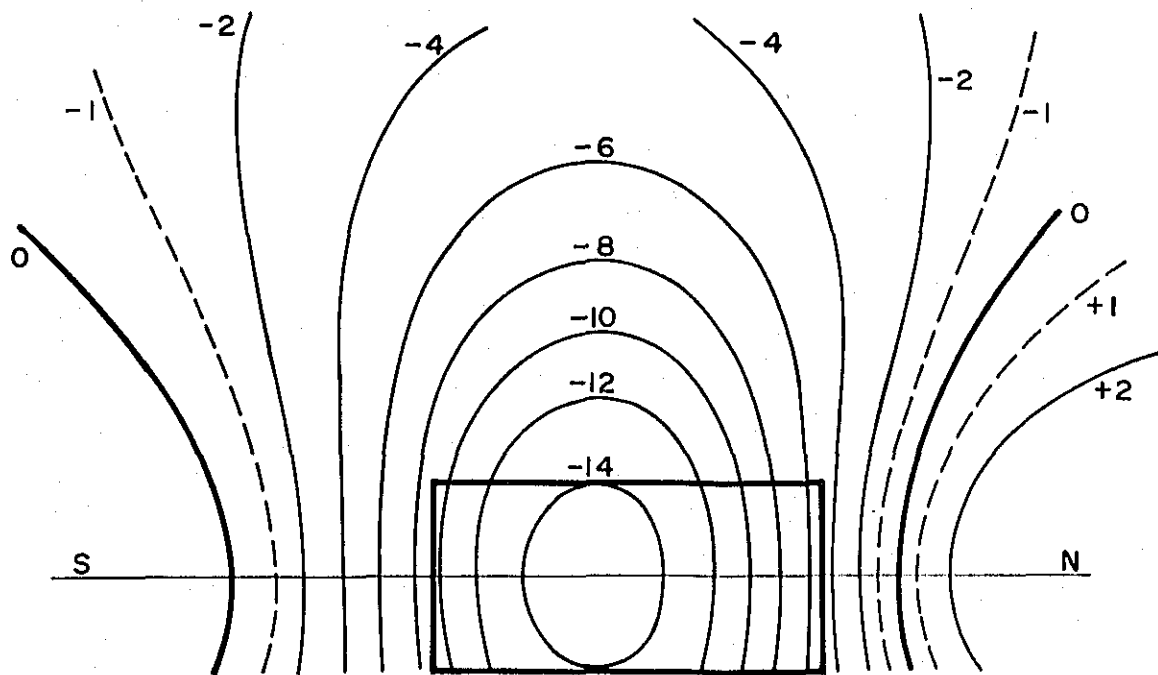


Fig. 6-8 Total magnetic anomaly by a prism model

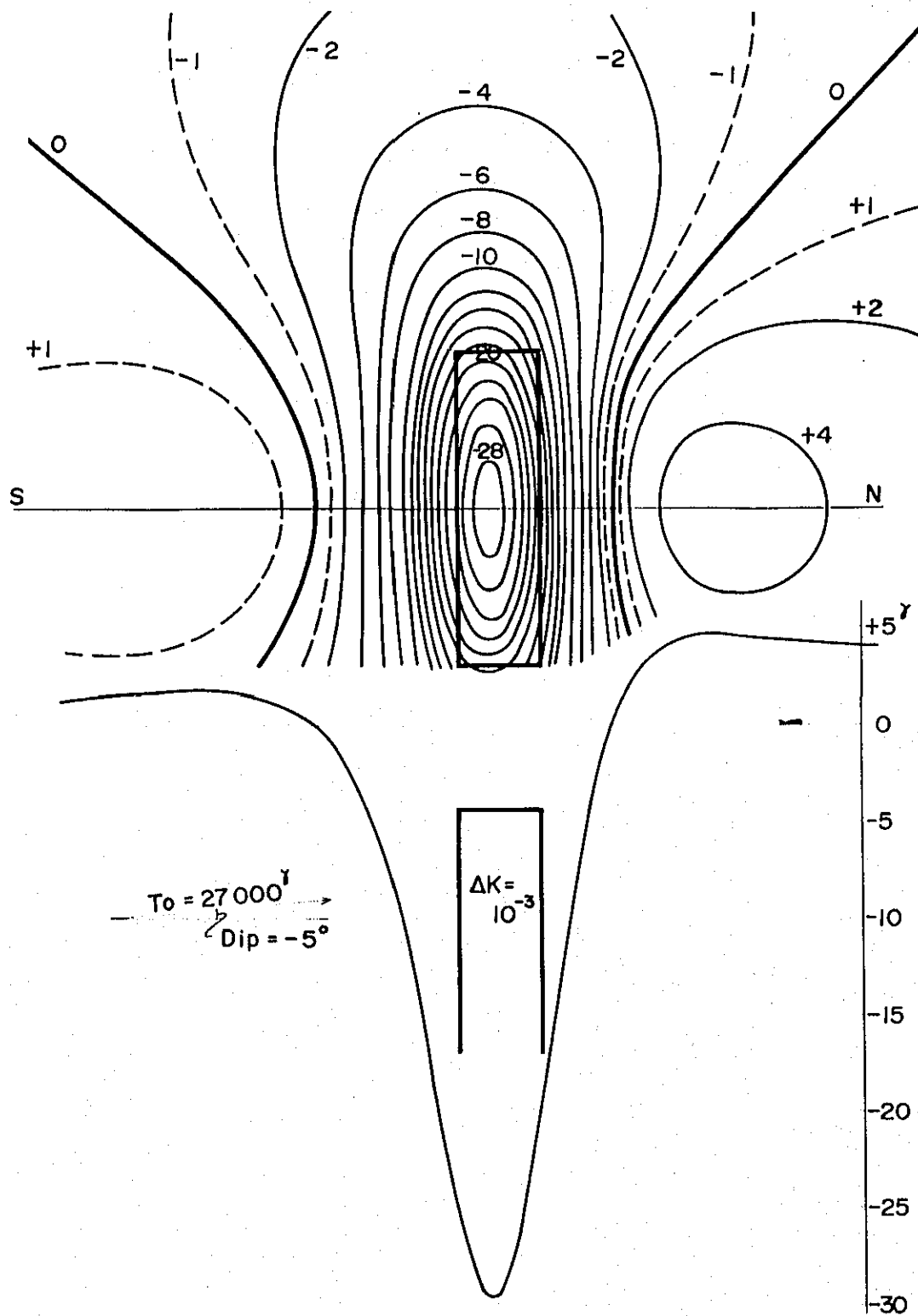


Fig. 6-9 Total magnetic anomaly by a prism model

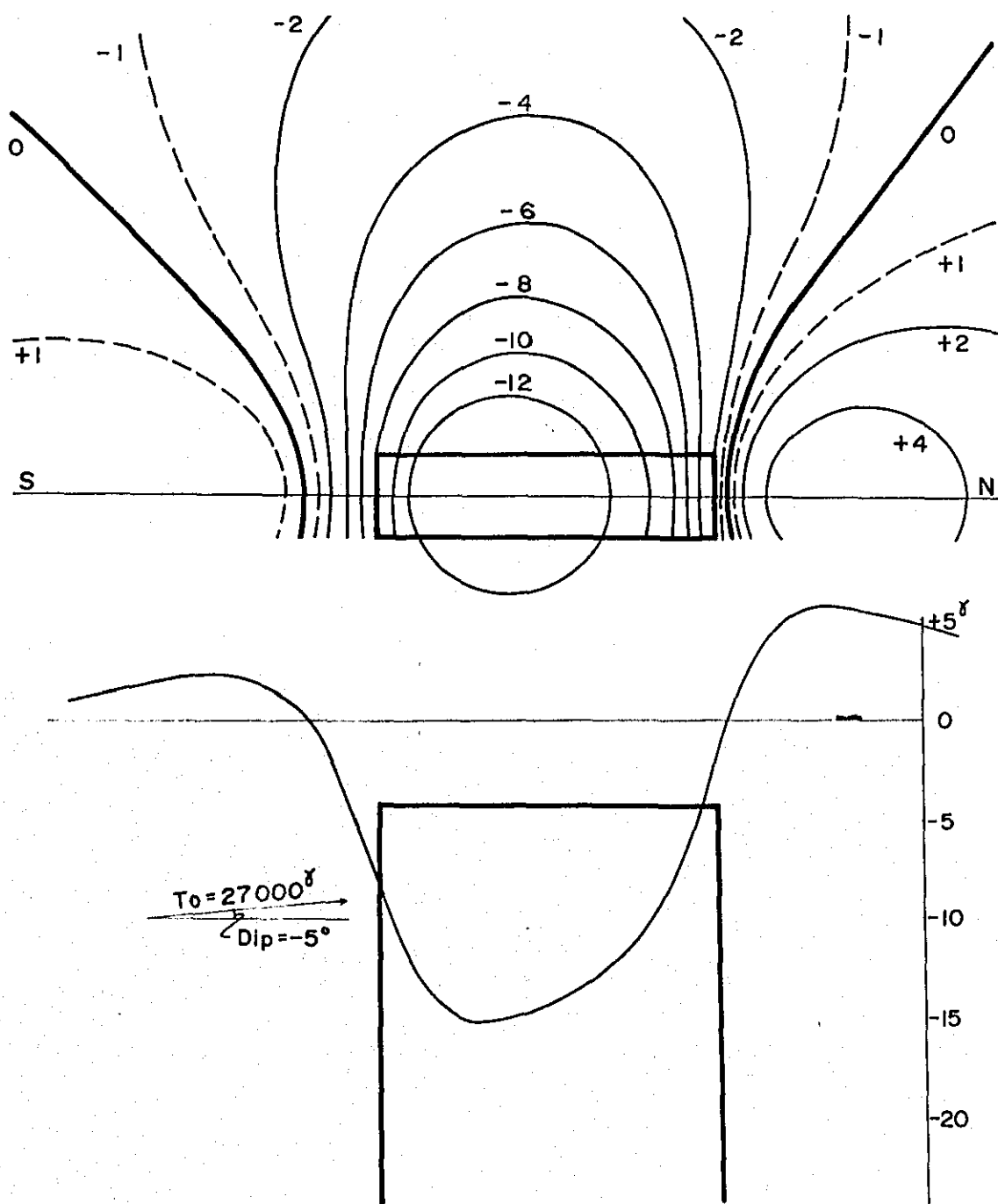


Fig. 6-10 Total magnetic anomaly by a prism model

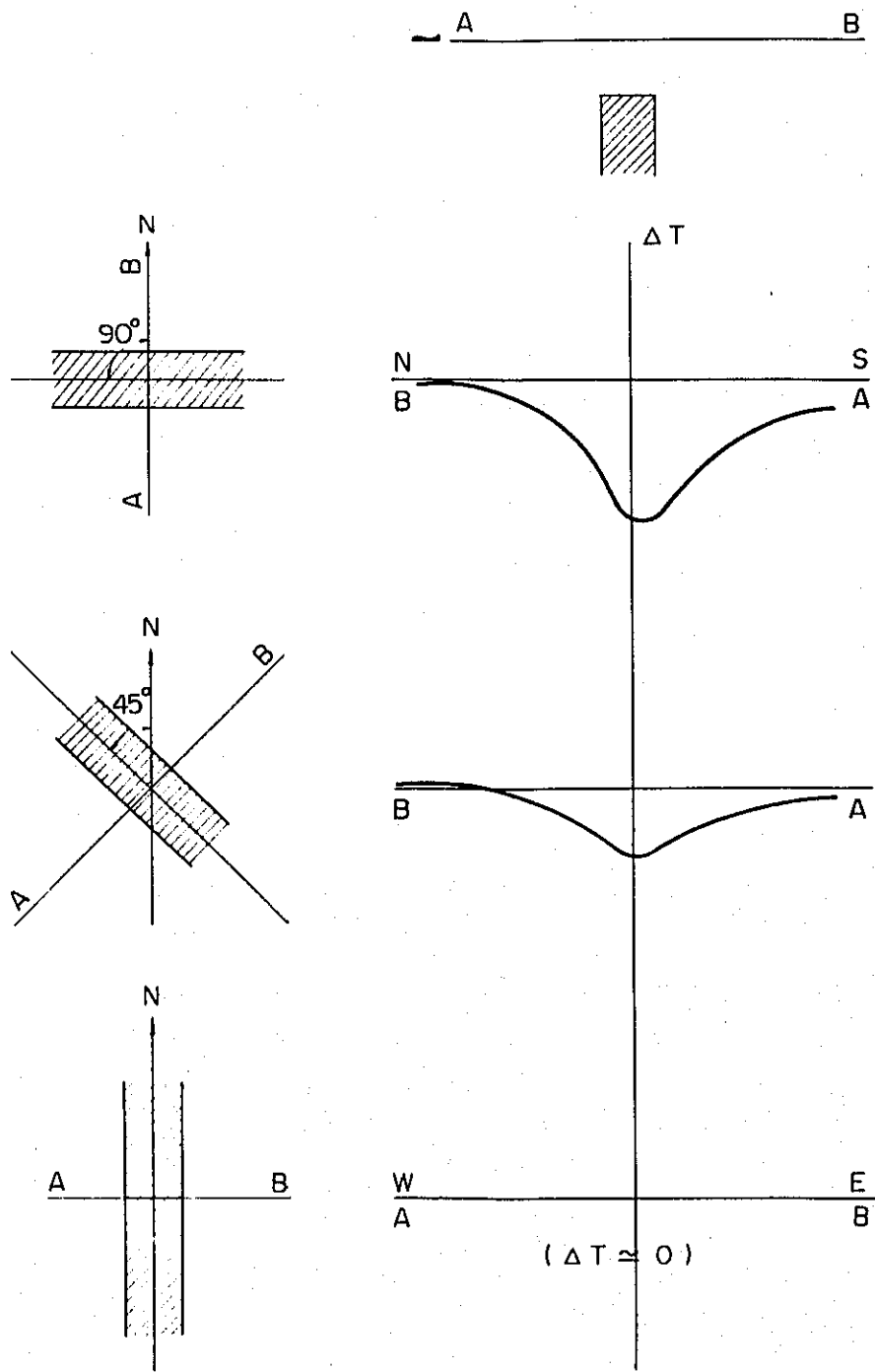


Fig.6-II Theoretical curves of total magnetic anomaly by dyke models

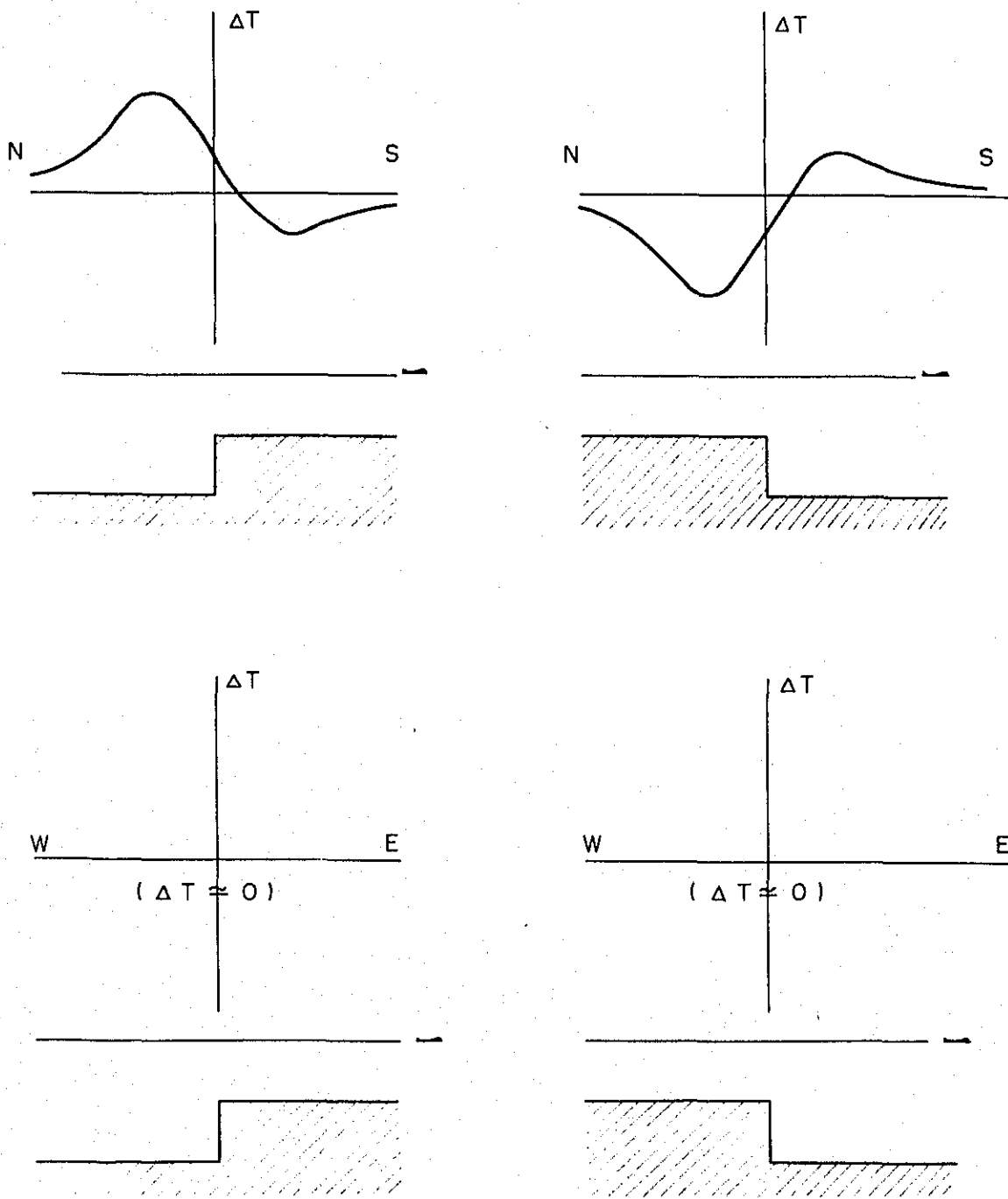


Fig.6-12 Theoretical curves of total magnetic anomaly by step models

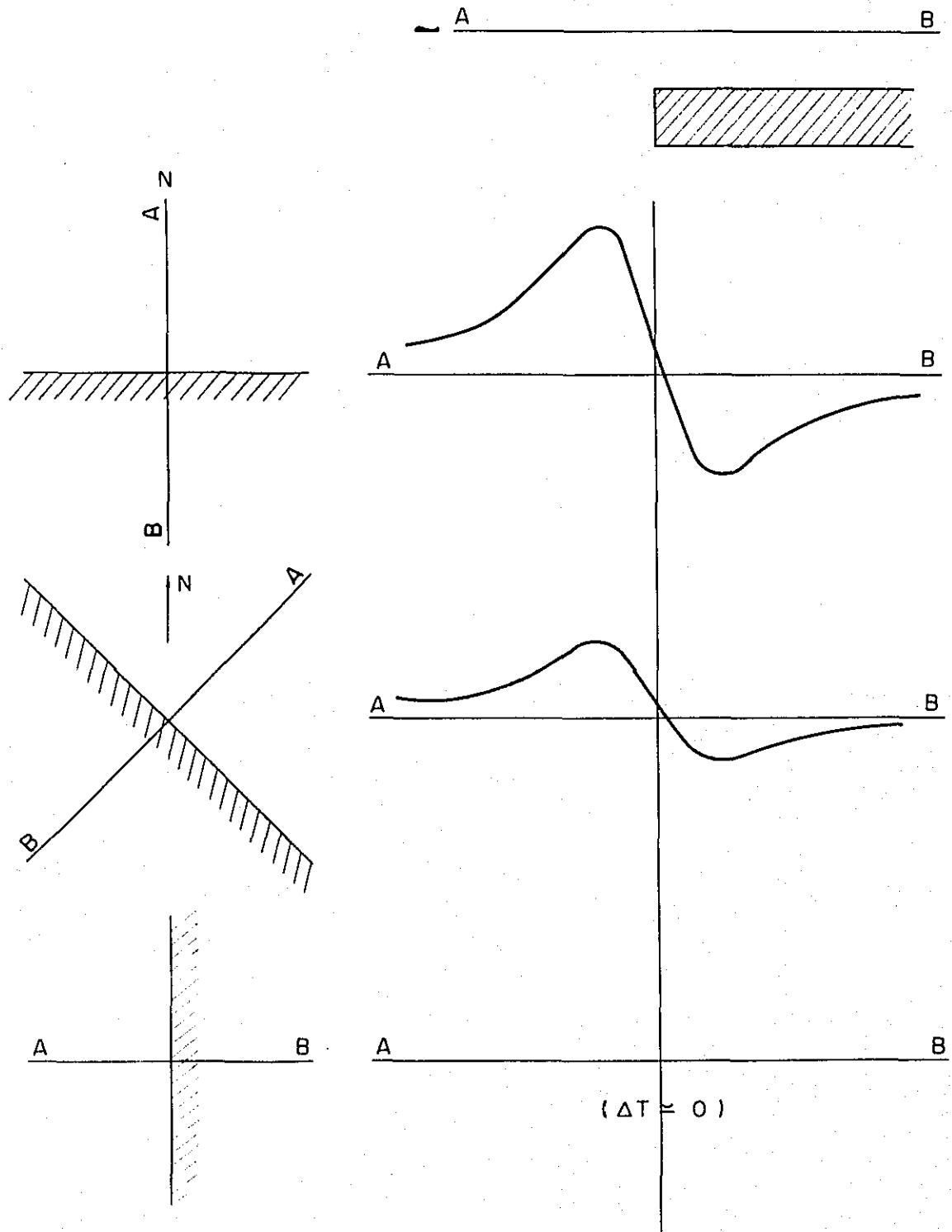


Fig.6-13 Theoretical curves of total magnetic anomaly by sheet models

7. INTERPRETATION

7-1 General Geology of the Surveyed Area

The general geology of the surveyed area is summarized as follows, based on the results of the photogeological survey and the ground geological survey in parallel with this survey. (ref. Fig. 7-1)

The area is roughly divided into two parts; the eastern part of the area forms basin, mainly consisting of sedimentary rocks, of the Mesozoic to the Quaternary period and the central to western part of the area forms mountains having such an high elevation of 4,000 m to 5,000 m, which consists of volcanic rocks, of the Tertiary to Quaternary period. And general trend of geological structure is NNW-SSE.

The explanation regarding the eastern part mainly consisting of sedimentary rocks, is made as follows:

- (1) The quartzite of the Lower to Middle Cretaceous (Yura Formation) exists in the zone between Rio Canipia and Rio Salado and in the vicinity of Velille.
- (2) Gray to black limestone (Ferrobamba F.) exists on the left side of Rio Canipia, in the zone between Rio Canipia and Rio Salado, and on the right side of Rio Salado.
- (3) Alternation of red sandstone and shale of the Upper Cretaceous (Capas Rojas F.) occurs widely in the north-eastern zone.

Granitic rocks (granodiorite, diorite, tonalite, and so on) intrude into these layers.

- (4) Volcanics, volcanic conglomerates, sandstone, and siltstone of the Lower Tertiary (Puno Group etc.) occur on the south-western and southern side of the zone as stated above in (3), bounded by faults.
- (5) Such sedimentary rocks (Barroso Group), as tuff, tuffaceous sandstone and breccia, of the Quaternary, being newer than those as stated above in (4), are present in this area (particularly, abound more toward the central part of the surveyed area).

In this group, (1) and (2) are marine sediments. The sediments (3), (4) and (5) are continentals consisted mainly of volcanic sediments and show belt-shaped distributions trending NNW-SSE.

In the central to western part, granitic rocks occur as the basement rocks, and the Tertiary volcanics (Sencca volcanics and/or Tacaza group consisted mainly of tuff to tuff breccia of dacite, basalt etc.) overlying the basement rocks, appears mainly in such valleys as located in the following:

- ① The region along Rio Velille and Rio Santo.
- ② The left side of Rio Yanama.
- ③ The vicinity of Chumpayo Lomas.
- ④ The region along Rio Pacapausa.
- ⑤ The region between Rio Jaculta and Colcahambe.

The Quaternary volcanics (consisting of the lava flows, tuff and tuff breccia of dacite and basalt, lava flows of the dacite and andesite, dacitic tuff to tuff breccia, lava flows and tuff breccia of the dacite, andesite and basalt — Barroso group), which overlie the Tertiary volcanics, occur almost over the area. Also the Upper Jurassic to Lower Cretaceous sedimentary rocks such as black shale and sandstone of the Yura formation occur over the narrow zone in the northern valleys.

The glacial deposits, fluvio-glacial deposits, and fluvial deposits, lying on the deposits so far mentioned, are distributed in the narrow zones all over the surveyed area.

These deposits are mainly distributed widely in the following regions:

- ① The upstream region of Rio Payacchuma on the north-eastern end of the surveyed area.
- ② Both sides of Rio Challuta.
- ③ The left side of Rio Jaro Mayo.

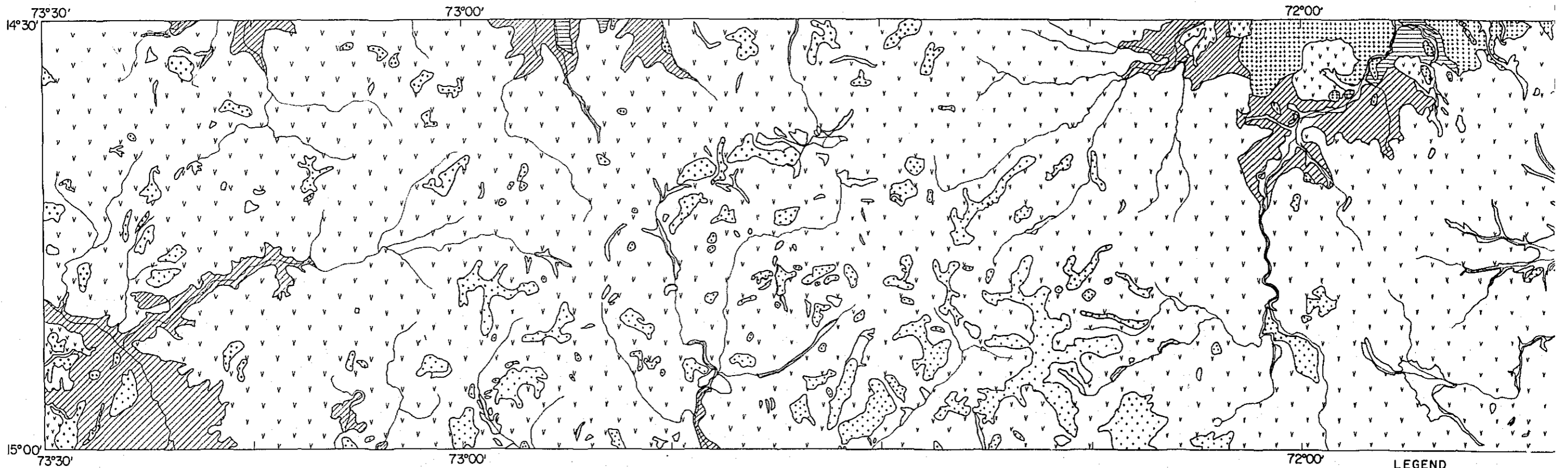
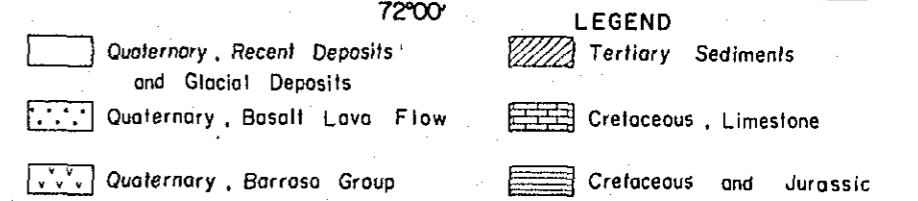
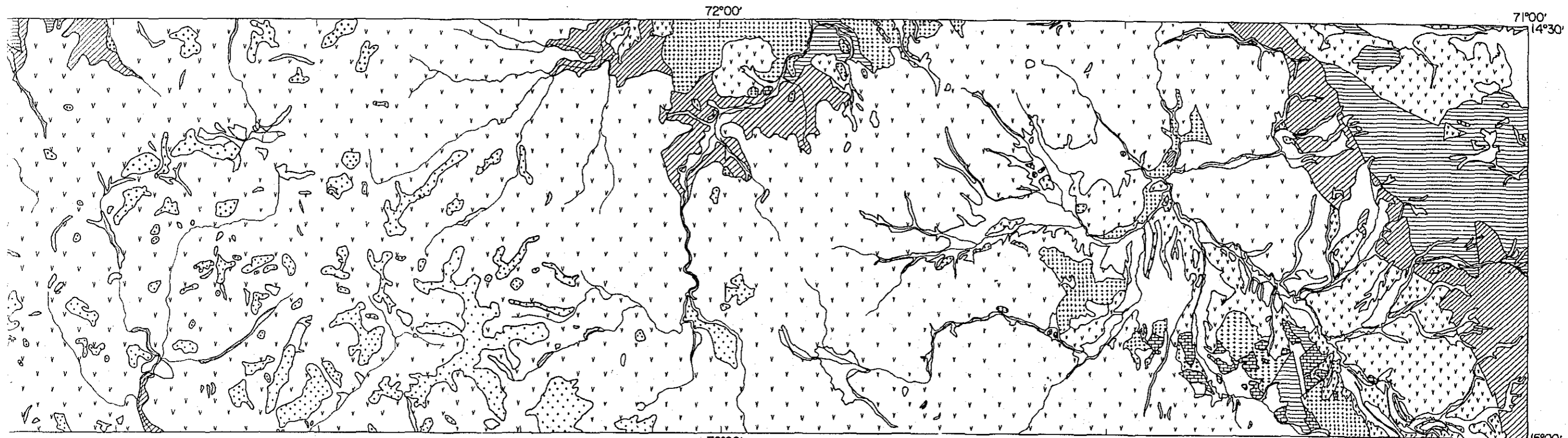


Fig. 7-1 General Geological Map








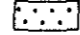
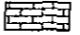
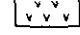
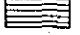
| LEGEND | | | | | |
|--|--|---|-----------------------------------|---|--|
|  | Quaternary, Recent Deposits and Glacial Deposits |  | Tertiary Sediments |  | Granitic Rocks (intruded into Pre-Tertiary rocks) |
|  | Quaternary, Basalt Lava Flow |  | Cretaceous, Limestone | | |
|  | Quaternary, Barroso Group |  | Cretaceous and Jurassic Sediments | | |

Fig. 7-1 General Geological Map

7-2 Analysis and Interpretation on Magnetic Data

The results of analysis and interpretation on magnetic data are shown on the following two types of interpretation map and on eleven magnetic profiles and sub-surface structures.

| | | |
|-----------------|--|---------------|
| MAP 7-1 & 7-2 | INTERPRETATION MAP OF NEAR-SURFACE MAGNETIC COMPONENT | S = 1:100,000 |
| MAP 8-1 & 8-2 | " | S = 1:200,000 |
| MAP 9-1 & 9-2 | INTERPRETATION MAP OF DEEP MAGNETIC COMPONENT | S = 1:100,000 |
| MAP 10-1 & 10-2 | " | S = 1:200,000 |
| FIGURE 1 ~ 11 | PROFILE A, B,, K | S = 1:200,000 |

Each location of PROFILE is shown on the Interpretation maps.

The interpretation on the near-surface magnetic component was made on the basis of the total magnetic intensity map (MAP 1-1 & 1-2) and the near-surface magnetic component map (MAP 3-1 & 3-2) and the interpretation on the deep magnetic component was made, based on the total magnetic intensity map (MAP 1-1 and 1-2) and the Deep magnetic component map (MAP 5-1 and 5-2).

The procedure required for these interpretations are shown in the followings.

- (a) Analytical works on the magnetic maps on the scale of 1/100,000 as listed above.
- (b) Sketch of magnetic trend as a measure of inferring the boundary, shape, of magnetic body, faults and so on.
- (c) Inferring the boundary, shape, of the magnetic body and the presence of faults based on the results obtained from the above item (b) and the features of magnetic anomalies.
- (d) Correlating of the magnetic maps with all the geological data and informations available.
- (e) Study on the relation between magnetic anomalies and these two factors of known ore bodies and intrusive rocks clarified by the photogeological analysis.
- (f) Obtaining the larger-scaled regional trend from the magnetic maps on the scale of 1/200,000.
- (g) Preparing the interpretation maps after the above-mentioned steps from (a) to (f) have been taken.

The analyzed results of both structures of near-surface component and deep component are mentioned later, and the magnetic characteristics of the surveyed area are explained as follows, based on the Total magnetic intensity maps (MAP 1-1 & 1-2).

A great number of magnetic anomalies form the complicated contour patterns, from which it is inferred that the surveyed area consists of volcanics zones, however, marine sedimentary rocks predominate in some parts of eastern half of the surveyed area. And most of anomalies are inferred to be caused by the magnetic rocks present in the near-surface, in the light of the wave length of the anomalies, and the anomalies caused by magnetic rocks present in the deep stratum are masked behind those caused by near-surface magnetic bodies, and there are few anomalies which can be easily recognized as attributable to the deep magnetic rocks. And in the surveyed area, there exist such parts where it is inferred that there is a strong contrasting relation between the patterns of the anomalies caused by the near-surface volcanics and the topography.

7-2-1 Interpretation on the Near-surface Magnetic Component

The magnetic rocks which are present in the near-surface and cause the magnetic anomalies are shown on "Interpretation map of near-surface magnetic component" (MAP 7-1, 7-2, 8-1 and 8-2).

According to the geological legend based on the analysis of photogeology, most of these rocks consist of volcanics of the Quaternary period, and then there are some anomalies caused by both volcanics of the Upper layer of the Tertiary period and granitic rocks of the Tertiary period. There are few anomalies caused by the rocks belonging to the Cretaceous and the Jurassic periods older than those rocks above-mentioned. The geology regarding the top of the magnetic rock existing in the near-surface, can be made clear, in comparison with the geological map drawn from the results of the photogeological analysis. Consequently, the average values of susceptibility contrast of magnetic rocks belonging to the identical geology shown on the above geological map can be obtained as shown below. In the case of the number of the magnetic rocks used for the calculation of the average value being small, the average values of susceptibilities thus obtained after calculation are not appropriate. However, the characteristics of magnetism of the geology in the surveyed area can be roughly inferred. The geology of the magnetic rocks and their average values of susceptibility contrast are shown as follows. (unit: $\times 10^{-3}$ c.g.s. e.m.u./cc)

| | | Note 1 | Note 2 | |
|------------|--------------------------------------|---|---|---------------|
| Quaternary | Recent | Lava Flow (Black Basalt) | 6.3 (18 pcs.) | |
| | Barroso Group | Upper | (Lava Flow or Tuff breccia of Andesite, Dacite, Basalt etc.) | 2.1 (11 pcs.) |
| | | Middle | (White tuff, Tuffaceous Sandstone, Tuffaceous Conglomerate, etc.) | 1.8 (6 pcs.) |
| | | | (White-Grey Dacitic Tuff, Tuff breccia) | 2.0 (12 pcs.) |
| | Lower | (Lava Flow, Tuff breccia and Tuff of Basalt, Andesite, Decite etc.) | 2.7 (36 pcs.) | |
| | | (Andesitic Tuff breccia) | 3.5 (7 pcs.) | |
| Tertiary | Sencca Volcanics and/or Tacaza Group | (Bedded Tuff, Tuff breccia of Andesite, Basalt etc.) | 3.0 (3 pcs.) | |
| | | Granitic rocks | 2.9 (5 pcs.) | |

Note 1 indicates the average value of susceptibility.

Note 2 indicates the number of the magnetic rocks.

The surveyed area can be tentatively divided into twenty zones according mainly to the direction of axes of the near-surface magnetic rocks and to the fault lines or magnetic discontinuity lines, and it can be inferred that there must have been some differences in the volcanic activity between each of several zones out of twenty ones as divided above. These twenty zones indicated by the alphabetical letters, such as A,B,C, can be classified into four groups as follows, based on the difference of the regularity specific in the respective arrangement of the near-surface magnetic rocks distributed on each zone.

| Direction of axis of magnetic rock | Name of zone | Fault (many or few) |
|---|--------------|---------------------|
| I WNW-ESE: many Rock's arrangement: regular | B2 | medium |
| | C1 | many |
| | C5 | " |
| | E1 | " |
| | E3 | " |
| II ENE-WSW: many Rock's arrangement: regular | C3 | medium |
| | C4 | " |
| | C6 | many |
| | D2 | medium |
| | E2 | few |

| | Direction of axis of magnetic rock | Name of zone | Fault (many or few) |
|-----|---|---------------|---------------------|
| III | WNW-ESE: half | B3 D4 G | medium |
| | ENE-WSW: half | | many |
| | Rock's arrangement: regular | | " |
| IV | Direction of axis: irregular Rock's arrangement: irregular | A | few |
| | | B1 | " |
| | | C2 | " |
| | | D1 | " |
| | | D3 | " |
| | | F | " |
| | | H | many |

The magnetic rocks are densely distributed in the group of I, II and III, but they are dispersed in the group of IV.

The aspect of the arrangement in the zone belonging to each group can be shown on such a model map as Fig. 7-2 "General trend of axes of near-surface magnetic rocks".

Judging from the above-mentioned general trend, in the western half part of the surveyed area, the near-surface magnetic rocks in each zone are distributed with such a directional trend as WNW-ESE or ENE-WSW, and it can be said that the cross-line made by both of the lines, one drawn by connecting roughly each zone in Group I and the other drawn by connecting roughly each zone in Group II, is similar to Type III as shown in Fig. 7-2, namely, general trend of axes of the near-surface magnetic rocks in Group III. It is inferred that these directional trends are related to the orogenic movement or the structure of the Andes.

Zone A is bounded on Zone B₁ and B₂ by Fault (a) and (b), and an obvious difference in the pattern of the magnetic anomalies is recognized, bounded on these faults. Namely, in Zone A, most of the anomalies having short wave length caused by the near-surface magnetic rocks do not form the closed contour lines, but the distorted ones only. In other hand, most of anomalies so caused in other zones form the closed contour lines. Therefore, magnetic pattern of Zone A is remarkably different from those of other zones. Most of these magnetic rocks causing distorted contour lines consist of tuff breccia of both andesite and basalt belonging to the Sencca volcanics and/or the Tacaza group of the Tertiary period, and the remaining ones consist of tuff of both basalt and andesite belonging to the Lower Barroso group of the Quaternary period.

A large-scaled anomaly observed in the center of this Zone A is caused by such magnetic rock present in the deep below ground surface as will be mentioned in section 7-2-2.

Most of the near-surface magnetic rocks causing anomalies in Zone, B₁ ~ B₃, C₁ ~ C₆, D₁ ~ D₄, E₁ ~ E₃ and G₁, consist of volcanics belonging to the Barroso group and of the Recent black basalt of the Quaternary

period. In Zone E₃, there exist a great number of anomalies caused by the black basalt. It is inferred that Zone, F, G and H are bounded by Fault, (j), (k), (l), (m) and (n), and that the volcanic activity of Zone G located between Zone F and H was most violent one of these three zones.

In addition to the anomalies caused by the volcanics of the Upper layer of the Tertiary and the Quaternary, in Zone F, there are several anomalies caused by a part of the granitic rock or contacted part between this granitic rock and the rock bordering on this granitic rock, on whose contacted part the magnetite is concentrated. These magnetic rocks are numbered as follows:

F-4, F-5, F-10, F-11 and F-13.

In Zone H, a great many anomalies are caused by the granitic rock or its contacted part on which the magnetite is concentrated and they are numbered: H-2, H-5, H-6, H-7, H-9, H-10, H-11, H-17, H-18, H-19, H-20, H-23 and H-24. And moreover, in this zone, there are many anomalies caused by the volcanics of the Quaternary period and by those of the Lower layer of the Tertiary period.

And also, in Zone H there exists the basin centering around Yauri and surrounded by Fault, (l), (m), (n), (o) and (p), and this basin forms a part of the vast basin extended from the Lake Titicaca east-south-east of the surveyed area. The magnetic anomalies caused by the granitic rocks are much abundant in the Yauri basin. It can be inferred from this fact that, in this basin, there is a great possibility of the occurrence of contact or porphyry copper deposit. From this point of view, two Zones, F and H, are the region where the discovery of new ore deposits can be more expected in comparison with the other zones.

It is recognized that the volcanic activity was very violent in the surveyed area as a whole, and it is also inferred from the magnetic survey that a great number of faults exist there, and most of them have the directional trend of NNW-SSE. This directional trend of the faults is thought to be ruled by the geological structure of the Andes.

Most parts of the surveyed area are covered with the volcanic rocks, some of which have a strong magnetism.

It is interpreted from this fact that the volcanic rocks greatly affected by the hydrothermal alteration caused by the violent activity of the volcanos, lost their magnetism, namely, the magnetite contained in the volcanics changed into oxide and sulfide, and as a result, it lost its magnetism, and it is inferred that a strong magnetism still remains in some volcanics which were not affected by the hydrothermal alteration. And it is supposed that there are some anomalies unable to be observed due to small thickness of the volcanics and to the wide clearance between the aircraft and the ground surface, even though the volcanics have magnetism.

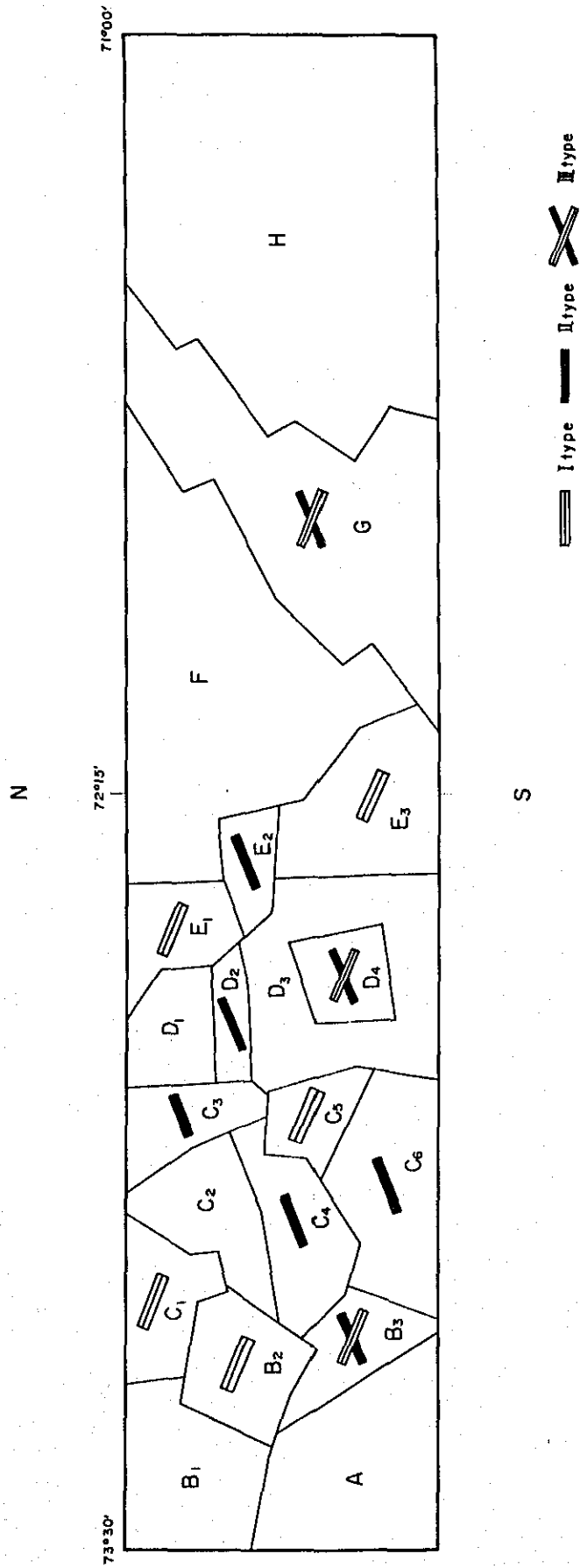


Fig. 7-2 GENERAL TREND OF AXES OF NEAR-SURFACE MAGNETIC ROCKS

7-2-2 Interpretation on the Deep Magnetic Component

As a analytical result of the deep magnetic components, the height above the sea-level, susceptibility contrast and rough shape, of the deep component magnetic rocks, are shown with their numbering, on the Interpretation map (MAP 9-1, 9-2, 10-1 and 10-2). The deep magnetic rocks consist of twenty-six, but more than half of them are distributed in the eastern half part of the surveyed area, and the size of the deep magnetic rocks is comparatively big and these big-sized ones are distributed in the direction from east to west, but the size of the magnetic rocks is small in the western half part of the area, and also these small-sized ones are distributed dispersedly and independently. Depth, susceptibility contrast, etc. of the deep magnetic rock are as shown on the Table 7-1, and their geology and features will be mentioned below.

The height from the sea level to the surface on the southern half part of Rock 1 has approx. 2,100 meters and the surface on its northern half is lowered with a fall of some 3,300 meters by a fault, and it is inferred that the eastern part of this rock bends to the south-east, caused by the fault running in the N-S direction, and it is further inferred based on the shape of the magnetic anomaly that Rock 1 forms a part of the large-scaled magnetic rock further extending to the west outside the surveyed area.

The height from the sea level to the surface of Rock 2 has approx. 1,400 meters, and a part of the south side is extruded upward, the top of which is about 3,600 meters high above sea level, and the central part of this rock narrows where a fault is supposed to exist. It is interpreted that both of Rock 1 and 2 may consist of the dioritic rocks.

Both tops of Rock 3 and 4 are approx. 3,600 meters high above sea level. Rock 5 has such a large value of susceptibility contrast as 8.5×10^{-3} c.g.s. e.m.u./cc, and there is the outcrop of the granitic rock at approx. 12 kilo-meters east of the center of this Rock 5 but no anomaly caused by this granitic rock can be observed. From this fact it is inferred that Rock 5 forms a partial extrusion of the basic plutonic rock, the rock facies of which is different from that of the outcrop of the granitic rock, and it is inferred that Rock 3, 4 and 5 consist of a partial extrusion of the large-scaled plutonic rock body lying in the deep below the ground surface, and that the difference of their susceptibility contrasts is attributed to that of their rock facies.

The top of Rock 6 lies near the ground surface at the elevation of 5,000 meters above sea level, but, based on the results of photogeological analysis, any plutonic rock does not occur in the region where Rock 6 exists. It is interpreted from this fact that this Rock 6 may consist of a huge massive volcanic rock. The eastern end of this Rock 6 is believed to be bounded on Rock 7 by a fault lying in between them. It is inferred that Rock 7 and 8 consist of plutonic rock -- probably dioritic rock --- based on their susceptibility contrasts.

Rock 9 has such a large value of susceptibility contrast as 9.0×10^{-3} c.g.s.e.m.u./cc and dips to the north. This Rock is interpreted

Table 7-1 Dimensions of deep magnetic bodies

| Rock No. | Situation (in meters) | | Susceptibility contrast ($\times 10^{-3}$ c.g.s.e.m.u./cc) | Notes |
|----------|---|-----------------|---|----------------------|
| | Below ground surface | Above sea level | | |
| 1 | 1,300~2,300 | 2,100 | 3.6 | Dioritic rock |
| 2 | 1,000~3,200 | 1,400 | 2.0 | " |
| 3 | 400 | 3,600 | 2.0 | Plutonic rock |
| 4 | 1,000 | 3,600 | 3.0 | " |
| 5 | 1,000 | 3,000 | 8.5 | Basic rock or Basalt |
| 6 | 0~200 | 5,000 | 1.4 | Volcanic rock |
| 7 | 1,100 | 3,900 | 2.0 | Plutonic rock |
| 8 | 700 | 4,100 | 4.4 | " |
| 9 | 900 | 3,600 | 9.0 | Basic rock or Basalt |
| 10 | 1,500 | 3,100 | 2.6 | Plutonic rock |
| 11 | 3,000 | 1,200 | 1.5 | Granitic diorite |
| 12 | Difficult to define the boundary of magnetic body | | | " |
| 13 | 500~1,000 | 4,000 | 1.2 | " |
| 14 | 1,500 | 3,200 | 1.3 | " |
| 15 | 3,500 | 1,200 | 1.4 | " |
| 16 | 1,500 | 2,700 | 1.9 | " |
| 17 | 2,000 | 2,200 | 3.2 | Dioritic rock |
| 18 | 3,000 | 800 | 3.0 | " |
| 19 | 2,800 | 1,800 | 2.2 | Granitic diorite |
| 20 | 1,000~2,100 | 3,300~1,900 | 1.1 | " |
| 21 | 400 | 3,500 | 0.7 | " |
| 22 | 100 | 3,900 | 0.8 | " |
| 23 | 400 | 3,600 | 2.1 | " |
| 24 | 4,000 | 0 | 0.3 | " |
| 25 | 900 | 3,700 | 2.8 | " |
| 26 | 800~1,000 | 3,400~3,200 | 0.3 ~ 1.3 | " |

to be composed of a basic plutonic rock or basaltic rock.

The top of Rock 10 is approx. 3,100 meters high above sea level, and the eastern end of this Rock is believed to be lowered by a fault.

It is inferred that Rock 11 is bounded on Rock 12 by a fault, but the boundary of Rock 12 is difficult to be exactly located because the magnetic data regarding the north side of Rock 12 is not available, but its southern boundary can be roughly located on the Map 9-2, as a result of the calculation from the data available regarding the southern part of Rock 12.

The wide granitic rocks are exposed to the ground surface, deep below which Rock 11 and 12 exist, and there is no magnetic anomaly caused by these granitic rocks exposed to the surface. From this fact, it is inferred that the rock facies of these granitic rocks vary as gradually as they deepen, therefore their magnetism seems to change accordingly, namely, being weak in the near-surface and strong in the deep, and it is interpreted that these granitic rocks exposed to the surface consist of the extruded parts of the deep magnetic Rock 11 and 12 which are believed to be composed of granitic diorite.

The top of Rock 13 is approx. 4,000 meters high above sea level and occurs below ground surface, ranging from 500 to 1,000 meters, and it is inferred that the northern part of this Rock is lowered with a fall of some 2,300 meters, and its eastern end is bounded on Rock 13' by a fault. These Rock 13 and 13' are also believed to consist of granitic rock.

Rock 14 dips to the north and is interpreted to be extruded from Rock 16.

Rock 15, 16 and 17 are distributed along the line in the east-west direction, and further on the north-east of Rock 18 bounded on the north-east end of Rock 17, Rock 23, 24 and 26 are distributed along the line in the north-east direction, and on the south-east of Rock 18, Rock 19, 20 and 21 are distributed along the line in the south-east direction.

Rock 15 dips to the south at an angle of approx. 70 degrees, and its east end is bounded on Rock 16 by a fault. The southern part of the top of Rock 16 is lowered in a shape similar to the steps, and it is inferred that Rock 14 is extruded from the deeper part of Rock 16.

Rock 17 consists of a fairly large-scaled rock body, and has the height of approx. 2,200 meters from the sea level to its surface, and is inclined to the south at a dip angle of approx. 70 degrees. The part adjacent to the north-east of Rock 17 is lowered by a fault, and it is inferred that this lowered part corresponds to Rock 18 and on the eastern side of this Rock 18, there exist Rock 19 and 23, which are extruded by a fault. From the susceptibility contrasts of Rock 17 and 18, it is interpreted that they consist of dioritic rock.

It is inferred that the difference in the height among the respective top of Rock 19, 20, 21 and 22 depends on each fault, and the difference

of the respective susceptibility accords with that of each rock facies.

The western part of Rock 20 dips to the north at an angle of approx. 45 degrees and also its eastern part dips to the north at an angle of approx. 70 degrees, and on the western part, this Rock's top is approx. 3,300 meters high above sea level and also its top dips to the east as high as approx. 1,900 meters above sea level.

It is inferred that the top of the northern part of Rock 22 is situated close to the surface and its southern part is lowered in a shape similar to the steps. It is believed that those Rock 19, 20, 21 and 22 consist of granitic diorite, but the susceptibility contrast of Rock 19 is a little greater than those of the other three.

Rock 23 dips to the north at an angle of approx. 20 degrees, and it is interpreted that there is no magnetism in its north-western part close to the ground surface, as shown in the attached FIGURE 8.

It is inferred that Rock 24 corresponds to a lowered part of Rock 26, and both western and eastern ends of Rock 24 are bounded on Rock 23 and 25 by the faults, and Rock 23, 24, 25 and 26 may also consist of granitic diorite, but the susceptibility contrasts of both Rock 24 and the western part of Rock 26 are comparatively small.

The southern part of the granitic rock distributed along Rio Aprimac passing on the west of Santa Lucia de Pichigua is believed to form an integral part of Rock 18 in the deep below the ground surface and it is also the case with its northern part forming an integral part of Rock 23, and it is inferred that the granitic rock distributed on the ground from the south of Coporaque to its west consists of a part extruded from deep magnetic Rock 17, and that the said rock distributed on the south-east of Yauri consists of extruded parts of Rock 19 and 20.

The granitic rocks distributed on the ground surface in the eastern half of the surveyed area are believed to consist of the parts extruded to the surface from the deep magnetic bodies, and it is inferred that the magnetic difference of these intrusive rocks depends on such factors as the composition of intrusive rocks at the time of their intrusion, the geological environment under which they are intruded, their weatherings and erosions. Particularly, the magnetism of these intrusive rocks is believed to vary vertically.

It is interpreted that these intrusive rocks are closely related to the occurrence of ore deposit, in spite of their existence in the near-surface or in the deep below the ground surface.

To grasp easily the large-scaled deep structure in the surveyed area, the distribution of deep component magnetic bodies and the height above sea level of their surfaces can be shown as a model map in Fig. 7-3.

Based on the height of the surfaces of these magnetic rocks, the whole area can be tentatively divided into three zones, such as "Zone I, II and III", as shown on Fig. 7-3.

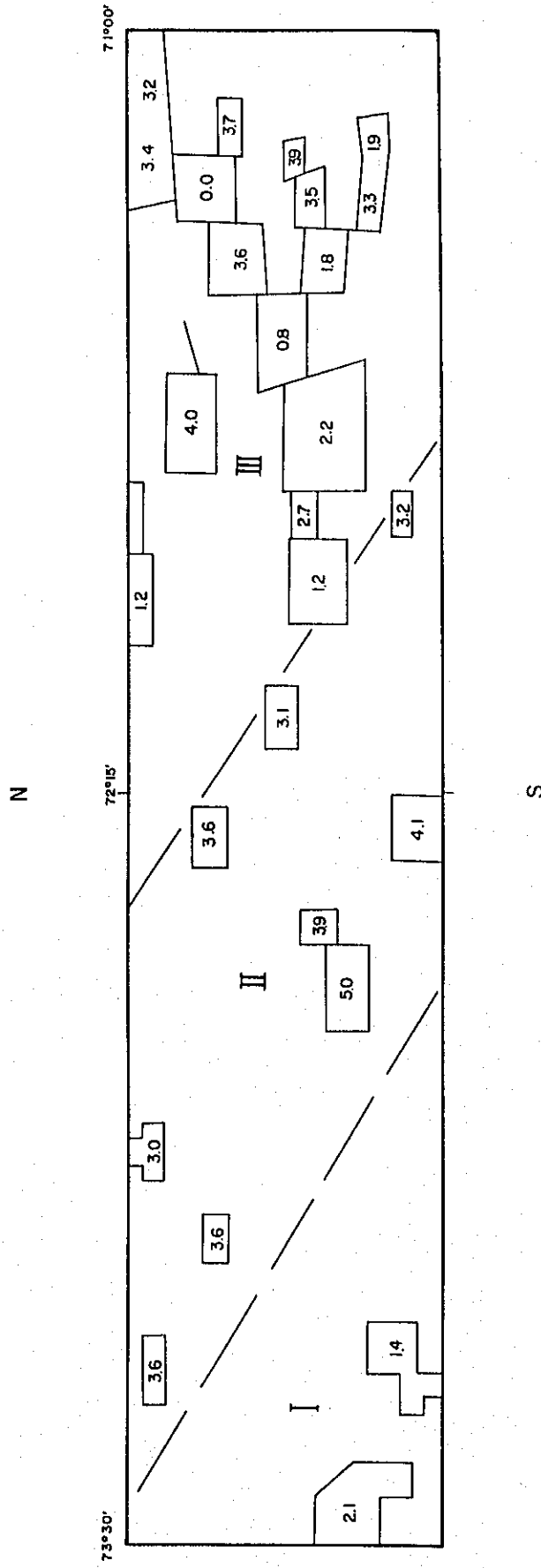


Figure shows height of magnetic body above sea level in X 1,000 meters.

Fig. 7-3 DISTRIBUTION OF DEEP COMPONENT MAGNETIC BODY

From the stand point of the plutonic rocks with strong magnetism only, the elevation of the plutonic rocks in Zone II is the greatest of these three zones. However, according to the results of the photogeological analysis, the granitic rocks are widely distributed on the surface in Zone III, but on the contrary, they are scarcely distributed on the surface in other two zones. Most of these granitic rocks exposed to the surface are distributed just above the place where the deep component magnetic rocks are present. It is inferred from this fact that the granitic rocks distributed on the surface consist of the extruded parts of the deep magnetic rocks. However, when the analyzed map of photogeology is compared with the Interpretation map of near-surface magnetic component, it is obvious that the area, totaling the parts showing magnetism in the granitic rock bodies exposed to the surface, is smaller than that, of non-magnetism. Therefore, both of the parts having magnetism and non-magnetism are believed to have homogeneous magnetism as their depths increase, and it is inferred that the only parts having the homogeneous magnetism in the deep are analyzed as the deep magnetic rocks.

The granitic rocks distributed in Zone III changes their rock facies vertically, therefore, the rock facies in the near-surface is believed to be granitic and that in the deep below surface is believed to be dioritic.

Considering the height of the surfaces of the plutonic rocks including such rocks having magnetism and non-magnetism as mentioned above, it is the greatest in Zone III and is approx. 4,000 meters above sea level. In other zones except III, few plutonic rocks are distributed on the surface, according to the results of the photogeological analysis, and even though the plutonic rocks are distributed below the surface, the presence of the plutonic rocks cannot be recognized from the magnetic survey only, if these plutonic rocks has no magnetism.

In order to interpret the three dimensional distribution of the plutonic rocks in Zone I and II, there is no alternative but to make the best informations regarding the deep component magnetic rocks obtained from the magnetic survey.

Therefore, reconsidering the height of the surfaces of the plutonic rocks present in the whole surveyed area on the basis of the above explanations relative to Zone I, II and III, it is inferred that the elevation of the tops of the plutonic rocks in Zone II and III, on an average, is almost the same and that the elevation of those in Zone I is smaller, compared with that in Zone II and III.

It is very difficult to interpret the horizontal connection between the respective plutonic rock in Zone I and II, because they are distributed dispersedly and independently, however, it is roughly interpreted that the deep component magnetic rocks are arranged as an axis of WNW-ESE and its arrangement seems to be undulated. It is inferred that the direction of this axis accords with that of the structure of the Andes. And many faults are believed to exist in the surveyed area, according to the Deep magnetic component map.

In Zone III, there exist many deep magnetic rocks, such as plutonic rocks, compared with those in Zone I and II, and also many intrusive rocks on the surface which are believed to be extruded from the deep magnetic rocks and to be closely related to ore deposits. Therefore, the further investigations should be conducted in Zone III.

REFERENCES

- (1) Dreyer, H. and Naudy, H., 1967,
Essai de filtrage non-linéaire appliqué aux profils aéromagnétiques:
Geophysical Prospecting V.16, No. 2, P.171
- (2) Mesko, G.A., 1966,
Two-dimensional filtering and second derivative method, Geophysics,
V.31, P.606-617
- (3) Darby, E.K., and Davies, E.B., 1967,
The analysis and design of two-dimensional filters for two-dimen-
sional data. Geophysical Prospecting, V.15, P.383-406
- (4) Rosenbach, O., 1953,
A contribution to the computation of "second derivatives" from
gravity data: Geophysics, V.18, P.46-71
- (5) Henderson, R.G., and Zietz, I., 1949,
The computation of second vertical derivatives of geomagnetic
fields: Geophysics, V.14, P.508-516
- (6) Oldham, C.H.G., 1969,
The $(\sin X)/X \cdot (\sin Y)/Y$ method for continuation of potential fields:
Mining Geophysics, V.2, P.591-605
- (7) Mufti, I.R., 1972,
Design of small operators for the continuation of potential field
data: Geophysics, V.37, P.488-506

